buildings

MDPI

Article

Mechanical Response in Existing Structure under Varied Subsurface Excavation Techniques

Jingwei Tong [1], Zihang Wang [1], Yichen Miao [1,2,*], Haiyuan Zheng [1,2,*], Yongchang Hu [1,2], Ruixue Li [1,2] and Peigen Tang [3]

[1] Faculty of Civil Engineering and Mechanics, Kunming University of Science and Technology, Kunming 650500, China; 2021618506137@stu.kust.edu.cn (J.T.); 2021618506238@stu.kust.edu.cn (Z.W.)
[2] Yunnan Seismic Engineering Technology Research Center, Kunming University of Science and Technology, Kunming 650500, China
[3] Baihetan Hydropower Plant, China Yangtze Power Co., Ltd., Ningnan 615400, China
* Correspondence: miao_yichen@kust.edu.cn (Y.M.); 20212210011@stu.kust.edu.cn (H.Z.)

Abstract: With the slowdown of urban incremental construction in China, reinforcement and renovation of existing buildings have become a hot topic in the fields of engineering and theoretical research. Underpinning pile foundations and underground excavation are commonly used methods for foundation renovation and reinforcement in existing buildings reinforcement and renovation projects. Nevertheless, there remains a dearth of relevant research concerning the effects of different excavation methods on the stability of existing structures during foundation reinforcement and underground space excavation. In the context of existing building pile foundation underpinning and underground excavation, this paper adopts a numerical simulation research method based on the modification of experimental model parameters, and it compares the overall stress changes and settlement of the underpinning pile foundation and the building under two modes of lateral and vertical excavation. The results indicate that there is a good agreement between the stress and settlement changes of the components in the indoor model experiment and the finite element simulation. Both excavation methods show that lateral and vertical excavation will generate maximum stress on the bottom components of the upper structure and the upper part of the pile. In terms of differences, vertical excavation will cause greater overall settlement of the building, but the settlement in different areas is basically the same. On the other hand, lateral excavation will have smaller overall settlement but may cause the structure to tilt. At the same time, lateral excavation will cause greater stress changes in the columns in the structure. Based on these findings, relevant engineering suggestions are provided to choose different excavation methods and strengthen existing buildings.

Keywords: existing structural reinforcement; underpinning; pile foundation; finite element analysis; excavation method; model test

Citation: Tong, J.; Wang, Z.; Miao, Y.; Zheng, H.; Hu, Y.; Li, R.; Tang, P. Mechanical Response in Existing Structure under Varied Subsurface Excavation Techniques. *Buildings* **2024**, *14*, 2008. https://doi.org/10.3390/buildings14072008

Academic Editor: Eugeniusz Koda

Received: 19 April 2024
Revised: 10 June 2024
Accepted: 25 June 2024
Published: 2 July 2024

1. Introduction

By 2050, it is projected that 68% of the population will reside in urban areas [1]. Many countries are experiencing a slowdown in new urban construction, and existing buildings are increasingly facing issues related to functional obsolescence and structural aging [2,3]. To address the growing urban population and the relative scarcity of building resources [4], retrofitting and strengthening existing buildings to extend their service life has become a hot topic in both engineering and theoretical research [5]. As the most crucial structural component, the foundation's strength and stability directly determine the lifespan of a building [6–8]. Therefore, exploratory research focused on the reinforcement and performance enhancement of existing building foundations plays a pivotal role in addressing the challenges posed by the increasing urban population [9]. To accommodate changes in building functions, extend the service life, and expand underground space, reinforcement, underpinning, and excavation beneath existing foundations are widely

used in practical engineering; they also bring new challenges to the design and research in this field.

With the rapid development of foundation underpinning technology in China, researchers have been increasingly deepening their application and innovation of related techniques through on-site studies [10,11]. Rossella et al. [12] used the example of a three-story underground parking lot in an urbanized area to explore the situation of flexible retaining structures in subsurface excavation conditions near existing masonry buildings. Dmochowski et al. [13] introduced a method of monitoring the settlement changes of an existing building's underground excavation conditions using a hydraulic leveling cell (HLC) system. They also discussed modern solutions for fixing existing building walls.

In the field of indoor model testing research, some scholars [14,15] have studied the changes in bearing capacity characteristics of foundations and the stability of buildings during foundation underpinning and underground excavation using small-scaled model tests. For instance, Yu et al. [16] conducted eight parallel scale model tests to simulate excavation and backfilling processes, studying the effects of excavation construction on adjacent buildings and surrounding soil. Zhang et al. [17] conducted two shake-table tests to investigate the influence of inertial load on the buckling behavior of rock-socketed piles partially embedded in saturated sands, and evaluated the inadequacy of current design codes in predicting the ultimate axial bearing capacity of pile foundations. Miao et al. [18] conducted model tests to reveal the changes in piles, beams, and columns over time during excavation, and studied the impact of underground expansion on the stability of the upper structure of an existing building.

Additionally, the use of finite element software to simulate and analyze the changes in bearing capacity and stress environment during the foundation reinforcement process of building structures has become an important method in theoretical research. In comparison with experimental studies based on traditional scale models, it avoids the influence of sample quality specificity and yields trial and research results that are more universally applicable for reference. Many scholars [19,20] have employed finite element software for specific application analyses. Lou et al. [21] established a 3D finite element model of a shield tunnel under an existing building and found that by increasing the radial injection radius of deep grouting and adjusting the scope of grouting reinforcement, the maximum lateral displacement of piles and the maximum settlement of the building could be effectively reduced. Xue et al. [22] used the finite element method to analyze the building foundation deformation under the condition of ultra-deep foundation excavation, and came to a consensus that effective basement support methods and pile reinforcement methods can effectively reduce the impact of the foundation pit on the building deformation. Li et al. [23] proposed a special component numerical analysis method to effectively explain the pile–soil interaction during excavation. San et al. [24] used Plaxis 3D finite element software to establish a model of the underground parking lot construction project in Gan Shui Village, Section 3, and analyzed the influence of different pile-cutting sequences on the bearing performance of the new foundation column. They found that the pile-cutting process had a significant impact on the bearing behavior of the structural column and the settlement behavior of the upper structure.

Due to the limitations of various objective factors in field experiments, the specificity of indoor model experiments, and the uncertainty in parameter selection of numerical simulation models, conclusions drawn from any single research method may be insufficient, especially in studies concerning the impact of different excavation methods on the stability of existing buildings. In response, we have adopted a numerical simulation analysis method based on the modification of experimental model parameters. Compared to traditional experimental research that relies on scaled models, a numerical simulation model adjusted with indoor experimental test parameters can effectively avoid the limitations of sample characteristics, resulting in findings that have broader applicability and reference value. Furthermore, in the aforementioned research, scholars conducted separate analyses on the stability of the superstructure and the bearing characteristics of the foundations

during underground excavation, yielding numerous valuable research outcomes. However, Harrington et al. [25] believe that in the process of analyzing the existing building pile foundation replacement and underground excavation using numerical analysis methods, the interaction between the upper structure, pile foundation replacement structure, and subsoil should be taken into consideration comprehensively. Studies on the differences in overall structural stability under various excavation methods remain scarce.

Our research team established a 1:10 scale physical experiment model, excavating the subsoil of an existing building through vertical and lateral methods, and comprehensively monitored the strain and settlement of the building's columns, beams, and piles during the excavation. The experimental model used particle concrete to construct the superstructure and acrylic as miniature underpinning piles to reinforce the foundation and expand the underground space. Using Abaqus finite element software and referencing indoor model test data, we established a three-dimensional finite element model for both vertical and lateral excavation based on experimental parameters. This model meticulously simulates the process of both excavation methods and explores their impact on building stability.

This article aims to analyze the impact of the internal force changes and settlement differences of existing buildings by two different excavation methods, lateral excavation and vertical excavation. As a result, recommendations for excavation methods are proposed based on the structural mechanical response of the building and site conditions. This also provides a basis for how to monitor and strengthen the existing structure.

2. Physical Model Test and Results Analysis

2.1. Model Design

In our study, we conducted experiments using small-scale models to simulate underground testing. The study is based on the simplification of a four-story mining structure in Chengdu. As depicted in Figure 1, the model was proportionally reduced to a scale of 1:10.

In Figure 1, the complete scaled physical model comprises two primary components. The upper part is a small frame structure model composed of fine steel wires and microconcrete, which is poured on-site during the testing process. Except for the bottom plate, the structural model is divided into four layers, with main dimensions of 900 mm in length and 750 mm in width. The aggregate height of the building above its base is 1500 mm. The first layer has a height of 600 mm, including a foundation embedding depth of 100 mm, while the second to fourth layers are each 300 mm in height. Furthermore, the lower section serves as a model settlement box.

The arrangement of instruments and the quantity of piles, columns, and beams can be observed in Figure 2. Strain gauges are positioned at the bottom midpoint of each beam, covering both the first and second floors within the structure. In the same way, strain gauges are placed at the midpoints of each column on both the first and second tiers. Furthermore, strain gauges are placed on either side of the pile, with the specific installation locations and spacing outlined in Figure 2a–c.

The excavation steps and areas for the two excavation modes are shown in Figure 3. In the diagram, the model box, soil, underground continuous wall, and micropile of the model test are labeled, along with the soil to be excavated in various stages, indicated by distinct colors and text. It should be noted that each color area in the figure is numbered once to represent the corresponding excavation stage of the soil in that area, and areas of the same color indicate that the soil was excavated in the same stage. For instance, considering the yellow zone beneath a solitary foundation in Figure 3a, this portion specifies that during stage VII of excavation mode 1, the entire upper half of the soil underneath the single foundation must be dug out.

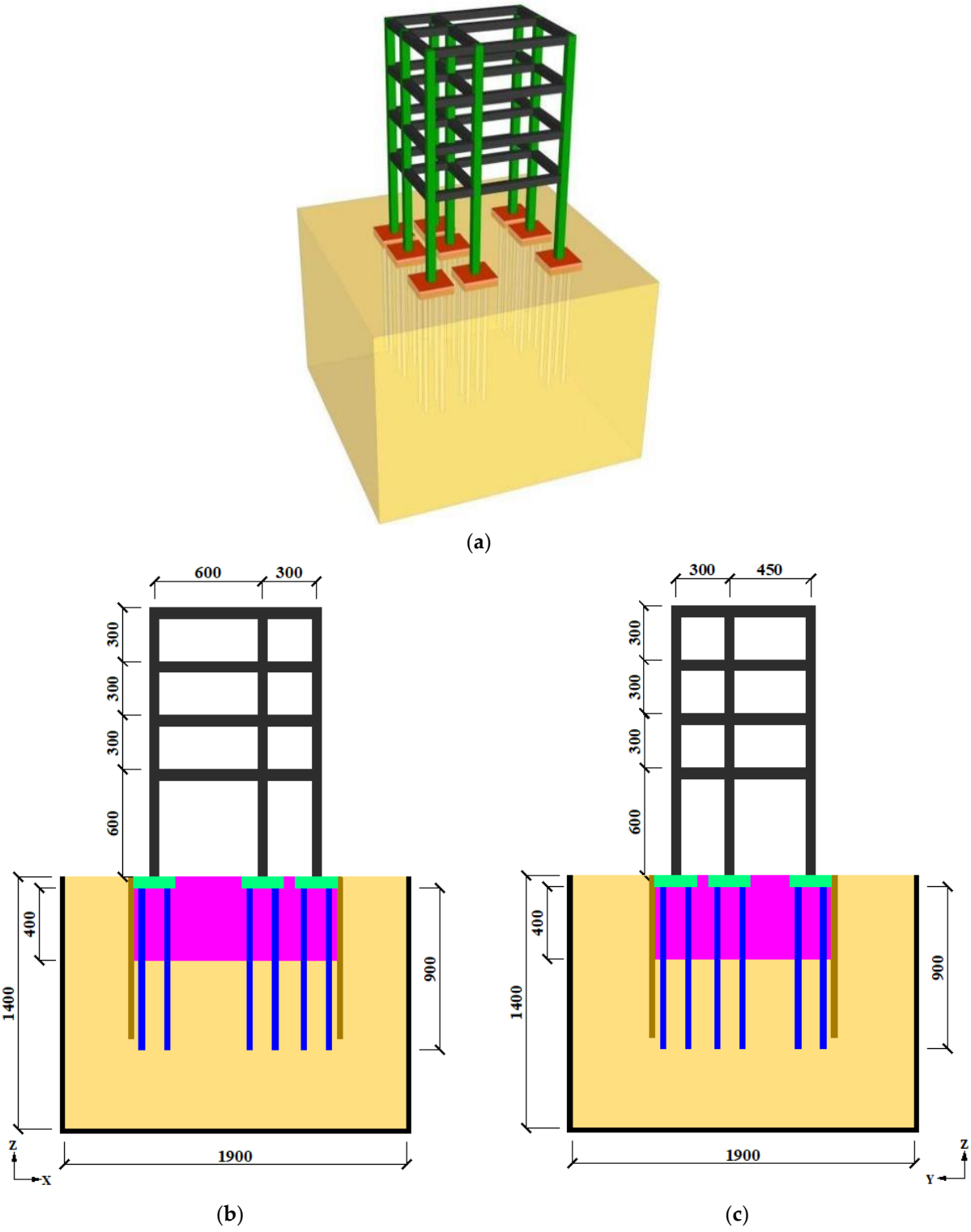

Figure 1. (**a**) Model test (the model scale is 1:10); (**b**) front view of model (Unit: mm); (**c**) side view of model (unit: mm).

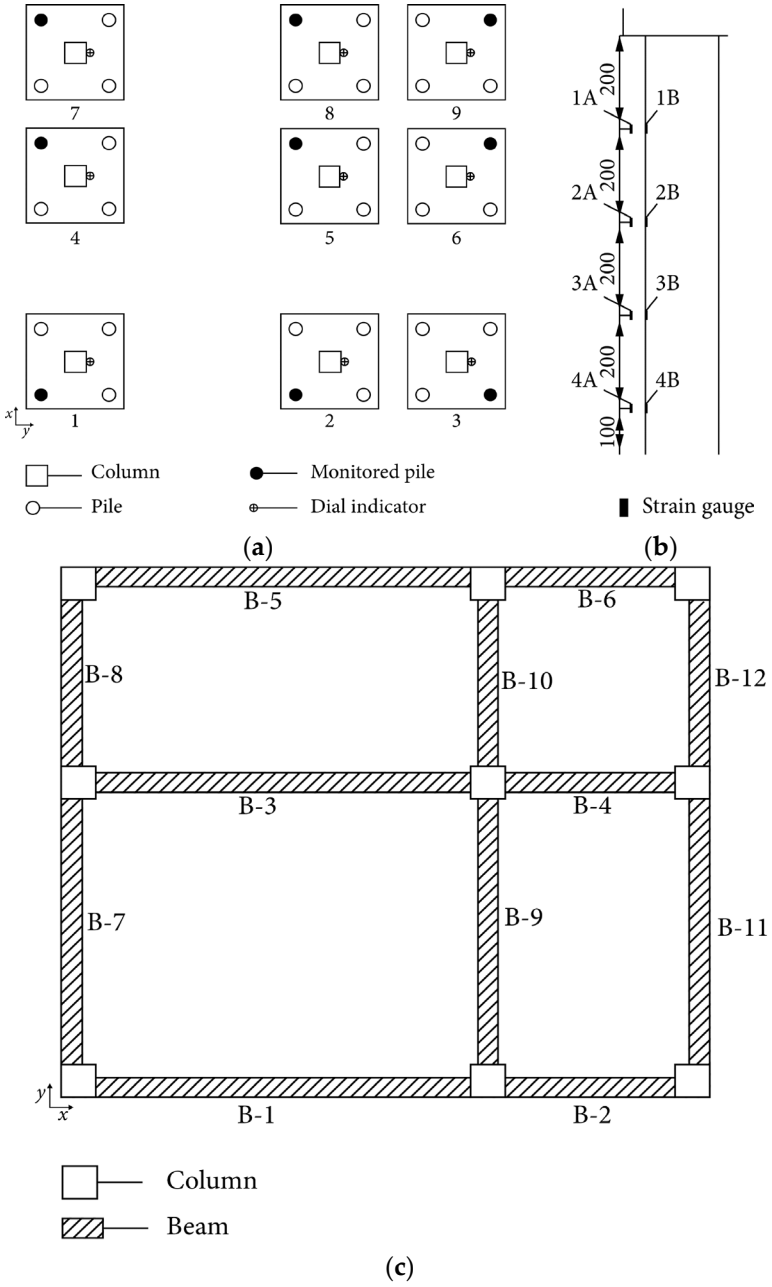

Figure 2. (**a**) Instrument setup plan; (**b**) layout of monitoring pile positions; (**c**) layout of number of crossbeams.

This study focuses on the differences in impact between two different excavation methods on existing buildings, with emphasis on each excavation stage. Therefore, the model assembly stage (I and II) is ignored, and stage III is considered the initial stage for analysis. Additionally, the strain changes in piles, columns, and beams, as well as the building settlement, are all caused by soil deformation. Therefore, in the analysis process, the underground part is analyzed first, followed by the above-ground part.

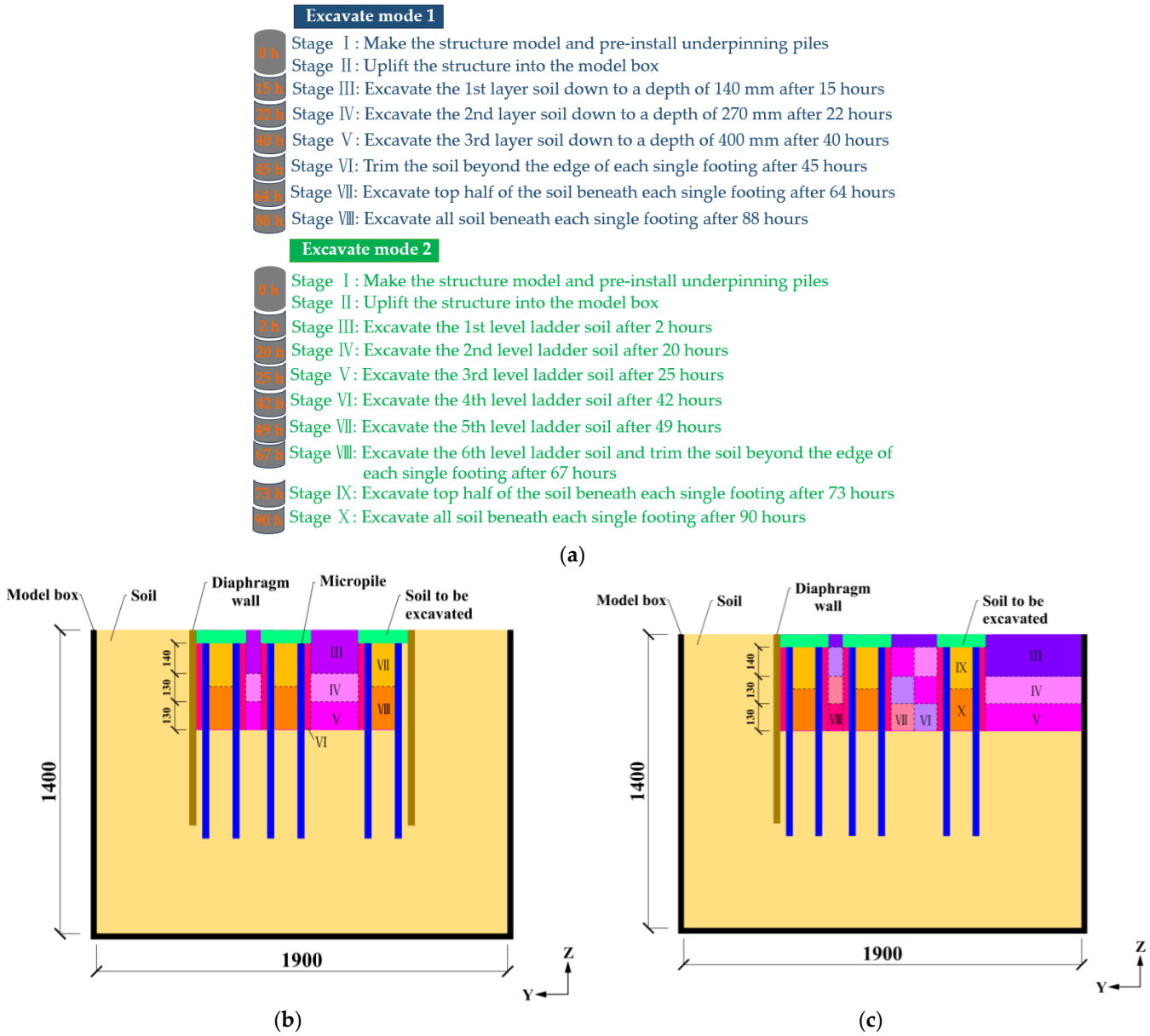

Figure 3. Excavation mode: (**a**) Excavation process; (**b**) excavation mode 1; (**c**) excavation mode 2.

2.2. Analysis of Underground Parts

2.2.1. Overall Settlement of Existing Buildings

In refs. [18,26], detailed analyses and explanations were conducted on the characteristics of structural force changes and building settlement rules, which is considered to be a supplementary explanation for the experiment. In order to obtain settlement data of the building, we installed strain gauges at the midpoint of the first and second floor columns. The recorded results are shown in Figure 4, where C1 represents column 1, C2 represents column 2, and so on. A positive sign signifies axial tension, whereas a negative sign signifies axial compression.

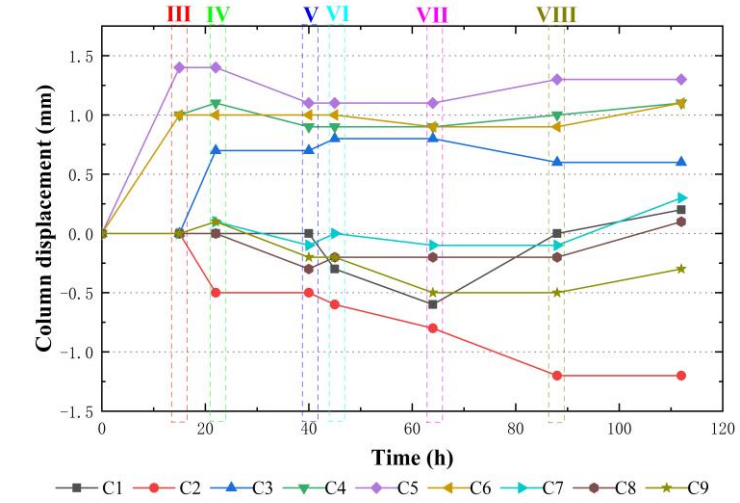

(**a**)

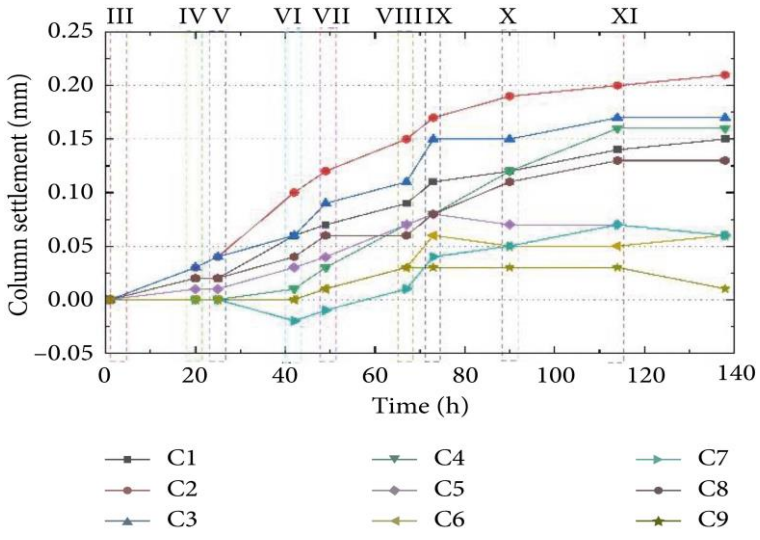

(**b**)

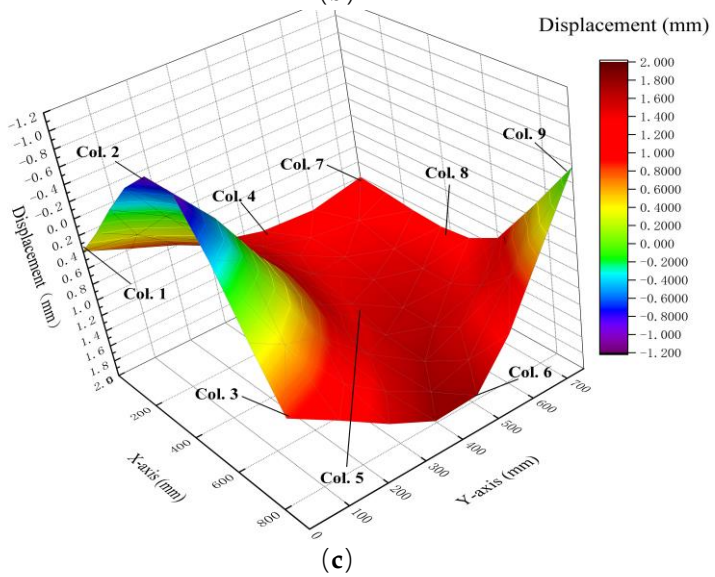

(**c**)

Figure 4. *Cont*.

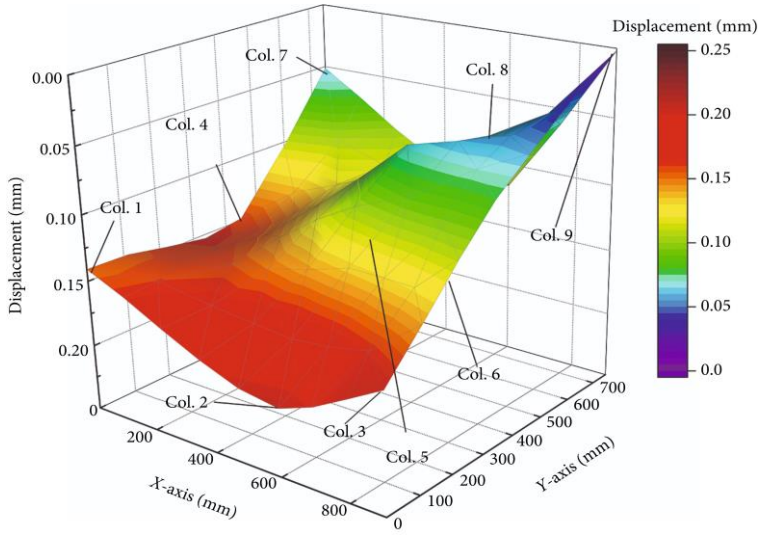

(**d**)

Figure 4. (**a**) Displacement of 9 columns in vertical excavation; (**b**) displacement of 9 columns in lateral excavation; (**c**) three-dimensional displacement of columns after 112 h in vertical excavation; (**d**) three-dimensional displacement of columns after 112 h in lateral excavation.

Figure 4a,b records the displacement changes of nine columns during two different excavation methods. Figure 4c,d respectively show the three-dimensional diagrams of the final settlement of columns under two different excavation methods. Based on the data changes, the following patterns can be determined:

(1) Analysis of the displacement trend: Under vertical excavation, all the columns exhibited significant displacement polarization. For example, columns C1, C2, C7, C8, and C9 experienced uplift during excavation, while columns C3, C4, C5, and C6 settled. This is because during soil excavation, some stress is transferred to the pile, causing settlement of the column. In addition, excavation can lead to stress unloading in the soil, aggravating this settlement trend. It is worth noting that columns subjected to larger forces often settle, while columns subjected to smaller forces may bulge. Under the lateral excavation method, except for the slight uplift of column 7 during the mid-excavation stage, all the other columns experienced settlement. The settlement values of each column using the lateral excavation method (maximum value: 1.40 mm) were considerably lower when compared to those using the vertical excavation method (maximum value: 0.21 mm).

(2) Analysis of uneven settlement degree: Under the vertical excavation method, the maximum settlement of the C5 column recorded in the first stage was 1.4 mm, while the maximum uplift of the C2 column in the eighth stage was 1.2 mm. The maximum uneven settlement after excavation was 3.5 mm. However, the settlement that occurred under lateral excavation is relatively uniform.

(3) Spatial distribution: Under vertical excavation, the central area along the X-axis usually showed higher settlement values, while the front and rear areas showed lower settlement values. Additionally, similar situations were observed along the Y-axis; under the lateral excavation method, the overall settlement sloped in a stepped manner towards the excavation side, showing a significant settlement value on the excavation side.

2.2.2. Changes in Pile Stress

Figure 5a,c shows the maximum strain values of piles at each stage under two different excavation methods. During the excavation process, some strain gauges of certain piles were damaged, and some of their data did not appear in the graph. To simplify the problem, only the absolute value of strain is being considered.

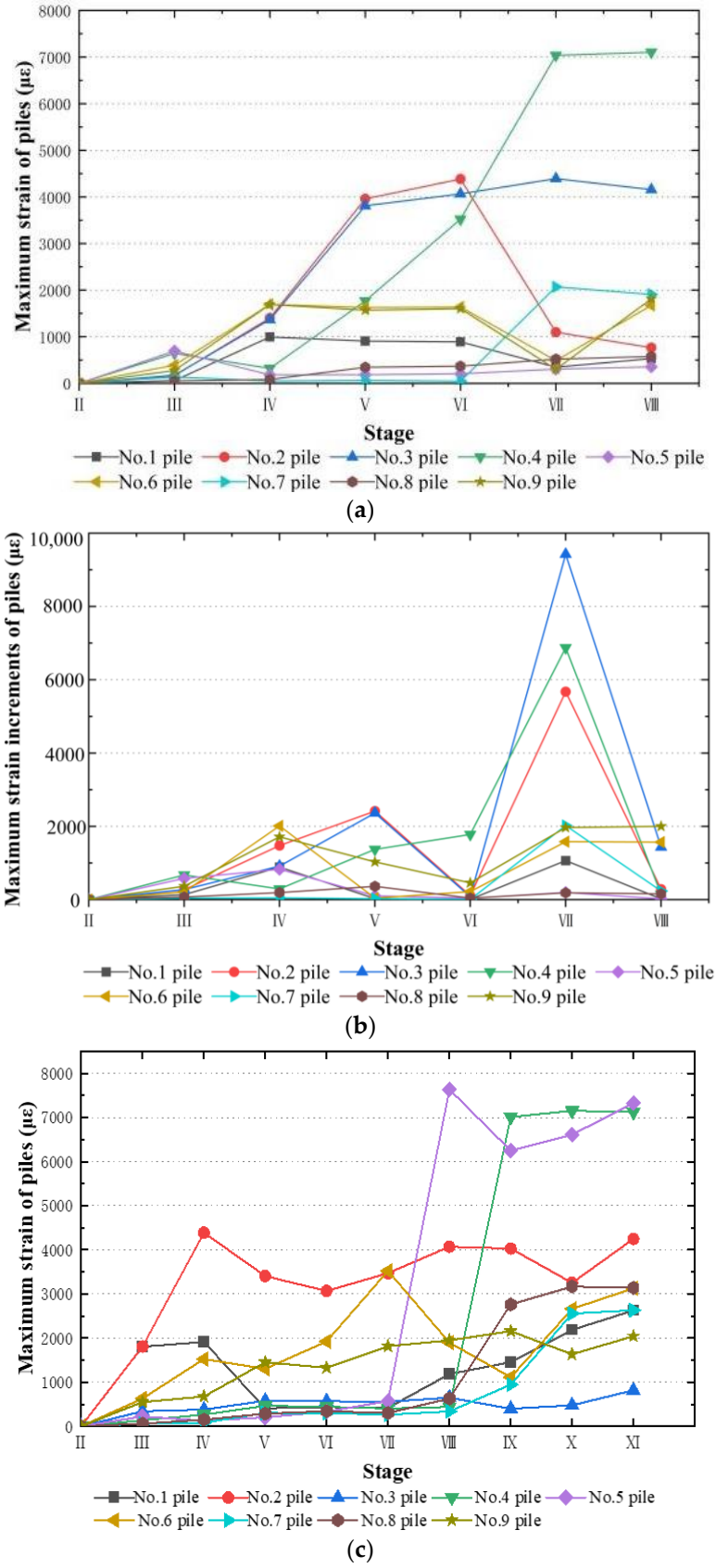

Figure 5. *Cont.*

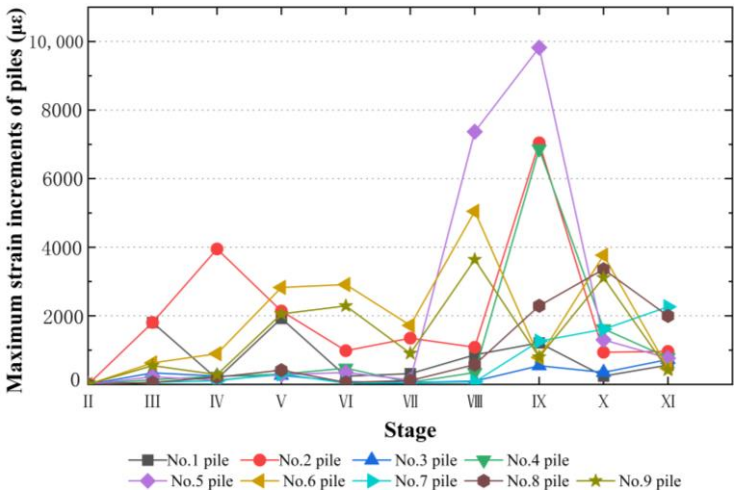

(**d**)

Figure 5. (**a**) Strain changes of nine piles in vertical excavation; (**b**) strain increment changes of nine piles in vertical excavation; (**c**) strain changes of nine piles in lateral excavation; (**d**) strain increment changes of nine piles in lateral excavation.

From the graph, the following can be seen:

(1) Under the vertical excavation method, as the excavation progresses, the maximum strain values of many piles experience an increase first, and then a decrease. Many piles experience a decrease in strain during stage VII, but at the same stage, the strain of the fourth pile actually increases to 7035 με, and the maximum strain difference between two piles is 6732 με.

(2) Under lateral excavation, the maximum strain value of the pile shows a fluctuating increase, with a slower increase in stages III to VII and a faster increase in stages VIII to IX. This could be due to the fact that during the initial stages of excavation, the soil underneath the foundation continues to endure the stress from the building above, and the strain variation resulting from excavation is comparatively minimal.

(3) In terms of the incremental stress for each stage, the two excavation methods have small changes in stress in the early stage, with the stress of the pile fluctuating slightly more in the vertical excavation condition. The incremental stress reaches its maximum value in the stage when the subgrade soil at the base of the abutment is excavated (the vertical excavation has a value of 9425 με, and the lateral excavation has a value of 9824 με), far exceeding other stages, especially in the lateral excavation.

2.3. Analysis of Aboveground Parts

2.3.1. Strain Changes of Columns

In refs. [18,26], the strain variation characteristics and rules of columns and beams are analyzed and explained in detail. Based on calculations derived from mechanical theory and engineering practice, the excavation process minimally affects the structure of the third and fourth floors of the upper building. Therefore, in the experiment, only the structures of the first and second layers were monitored. The maximum strain values of columns in different layers during each excavation stage under two excavation methods are shown in Figure 6.

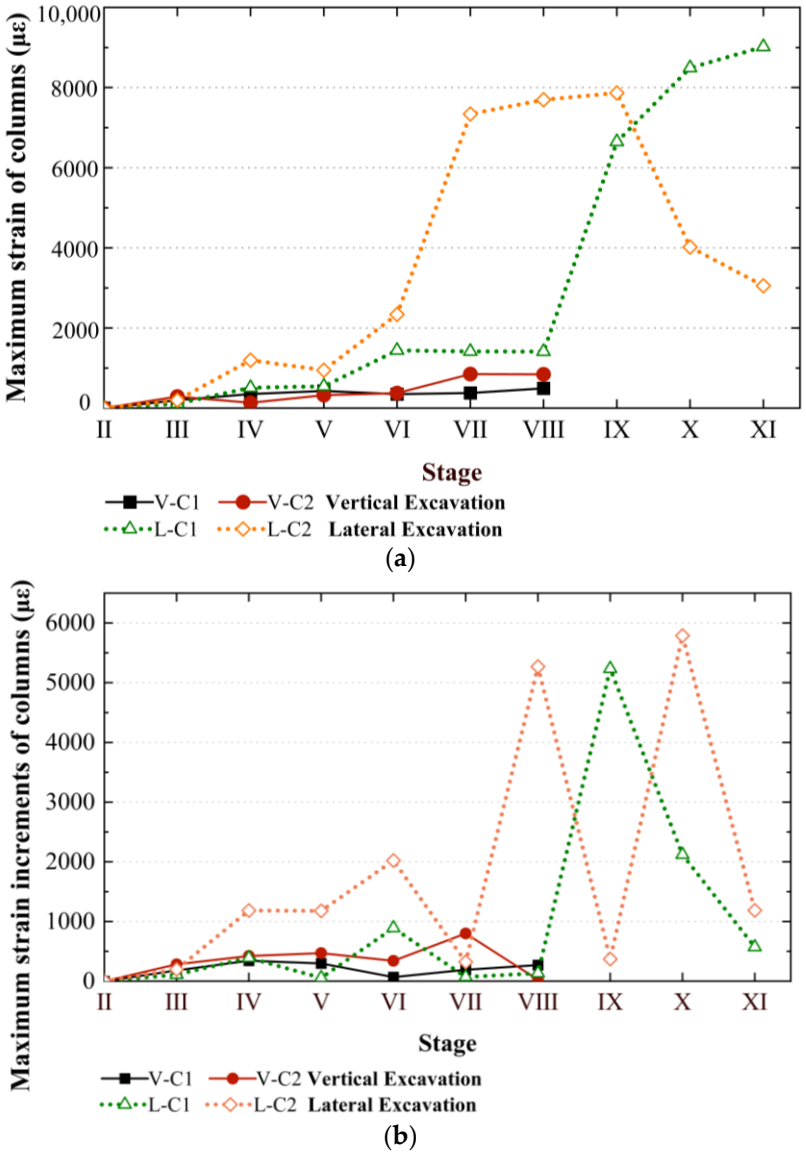

Figure 6. (**a**) Maximum strain of columns; (**b**) maximum strain increments of columns.

Based on the monitored column strain data, the following patterns were observed: (1) The maximum strain values of the columns fluctuated at each stage of the two excavation methods. Under the vertical excavation method, the most significant strain changes in the first layer of columns occur in stages VII and VIII, which may be due to the sensitivity of the columns to the soil height under each foundation angle, and these stages involve excavation of the soil under each foundation. However, excavation in stages VII and VIII has a relatively small impact on the strain fluctuation of the second layer column, indicating that the excavation of the lower soil of the foundation has little effect on the strain of the upper column. Under the lateral excavation method, the most significant strain changes of the two columns occurred in stages VIII and IX. However, in stage IX, the strain changes of the two columns were opposite. The strain of the first column decreased significantly, while the strain of the second column increased significantly. This may be related to the stress redistribution caused by the soil below the excavation foundation angle. (2) There is a notable discrepancy in strain values among the two layers of columns when considering two different excavation methods. Under vertical excavation, the strain values of the first- and second-layer columns are relatively close, and both fluctuate within a small range. Under the lateral excavation method, there is a significant difference in the strain values between the first- and second-layer columns in the later stage of excavation.

Figure 6b shows the maximum strain increment of columns at different stages under two excavation methods. (1) Under the vertical excavation method, the strain increment of the two layers of columns slowly increases with the excavation process. When the excavation reaches stage VI, the maximum strain increment of both layers decreases, but overall, the maximum strain increment in both layers remains very similar throughout the excavation process. Secondly, in the eighth stage, the maximum strain increment of the second layer column reaches its peak at 799 με. (2) Under the lateral excavation method, the maximum strain increment of the two layers of columns shows a fluctuating upward trend, but the numerical difference is more obvious. In stage X, the maximum strain increment of the second layer column reaches its peak at 5787 με, and the maximum strain difference with the first layer column in this stage is 3667 με.

2.3.2. Strain Changes of Beams

The beam's strain gauges are positioned on the structure's first and second layers, respectively. The strain record of the first layer beam under vertical excavation method is V-B1, and the strain of the second layer beam is called V-B2. Under the lateral excavation method, the strain record of the first layer beam is L-B1, and the strain of the second layer beam is called L-B2. Finally, a positive sign indicates axial tension, and a negative sign indicates axial compression.

Figure 7a shows the maximum strain values of beams at different stages under two excavation methods. To simplify the problem, the figure only considers the absolute value of strain and only provides the maximum strain value of the beam at each excavation stage. (1) Under the vertical excavation method, as the excavation progresses, the maximum strain values of the first- and second-layer beams show an upward trend. In addition, the strain value in the second layer is smaller than that in the first layer. The first-layer beam has the highest strain in stage VII, which is 6092 με. The maximum strain difference between the two beams reaches 3802 με. (2) Under the lateral excavation method, the maximum strain values of the two layers of beams gradually increase and the difference is small. However, in the XI stage, the strain of the first layer of beams reaches its peak, which is 6047 με. The maximum strain difference between the two beams reaches 3029 με. Therefore, regardless of the excavation method used, the first layer of the beam is more prone to damage during the excavation process.

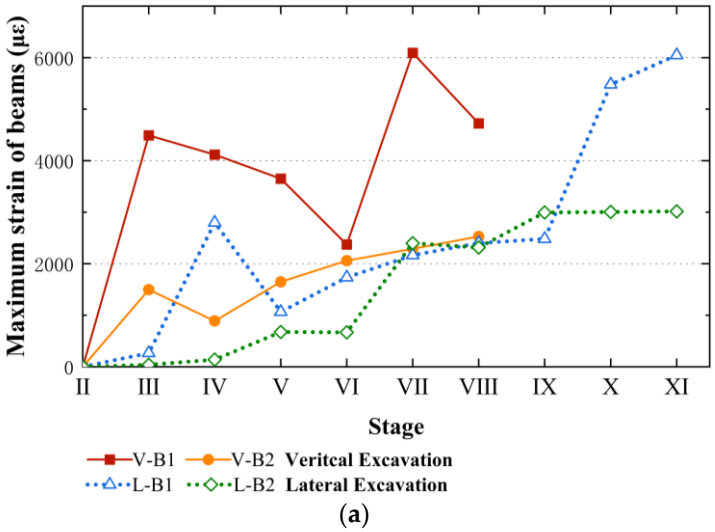

(**a**)

Figure 7. *Cont.*

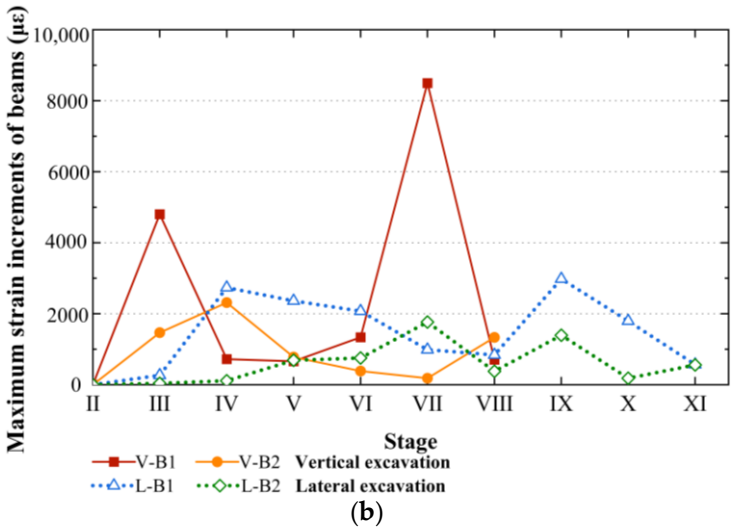

Figure 7. (**a**) Maximum strain of beams and (**b**) maximum stain increments of beams.

Figure 7b only considers the absolute increment of beam strain for each excavation stage under two different excavation methods. (1) During vertical excavation, the increase in strain in the first layer is significantly greater than that in the second layer. In the seventh stage, the first-layer beam experiences the highest strain increment, reaching 8496 με. The second-layer beam's strain increment at the same stage is merely 182 με. The strain difference between the two beams is 8314 με. The first-layer beam is more prone to damage. Secondly, in addition to the seventh stage, the first-floor beam also generated strain increments of 4802 με in the first stage. This also hinders the stability of the framework. (2) During lateral excavation, the strain fluctuation in the first-layer beam is higher than that in the second-layer beam. However, when compared to vertical excavation, the strain difference between the two layers of beams is smaller, and the change trend is similar.

2.4. Strain Analysis at Structural Spatial Positions

Figure 8a,b depicts the spatial distribution of strain changes within the structure under two different excavation methods using the absolute values of internal strain. It should be noted that according to the calculation results obtained from mechanical theory and engineering practice, the excavation process has a relatively small impact on the structure of the third and fourth floors of the upper building. Therefore, in the experiment, only the structures of the first and second layers were monitored. Overall, during the experiment, it was found that the two excavation methods have the following characteristics:

(1) Under both excavation methods, the total strain value of the first-layer structure exceeds that of the second-layer structure. The peak strain of the column is relatively low and occurs at external positions. Therefore, it is necessary to reinforce the first-layer beam and consider reinforcing the columns and the second-layer beam.

(2) In the later stage of excavation using both excavation methods, the upper frame structure and piles showed the highest strain values. This phenomenon is attributed to uneven settlement after excavation, resulting in stress redistribution throughout the entire structure. Therefore, high-strength prefabricated piles must be used as support elements to withstand the complex strain changes and adverse excavation conditions of the piles. In the later stage of excavation, the excavation speed should be appropriately slowed down, such as by further refining the excavation area into smaller blocks, in order to alleviate the stress redistribution process within the entire structure.

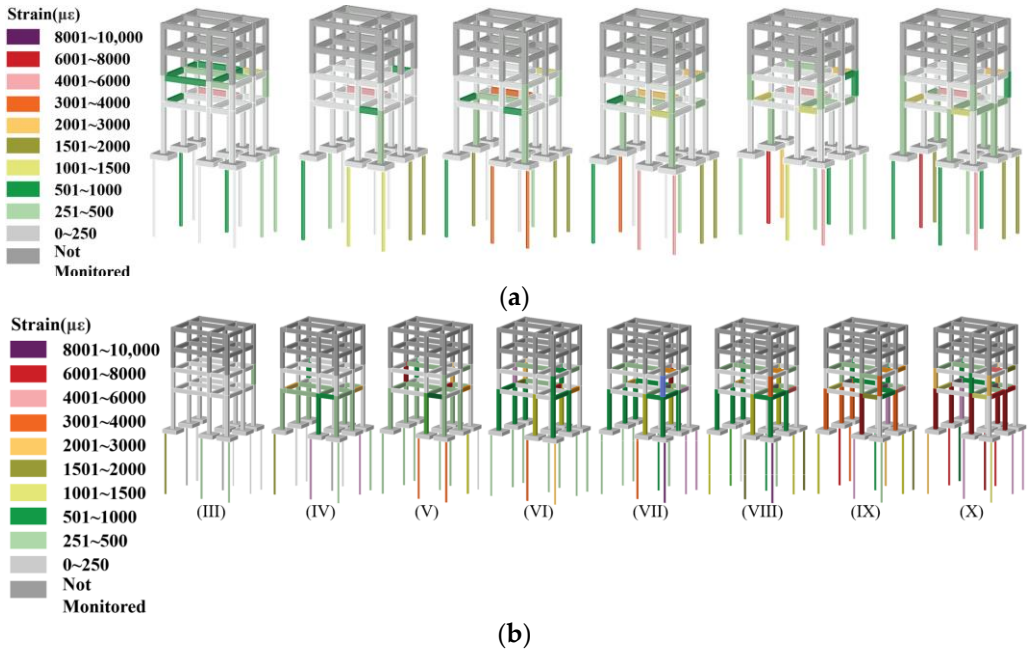

Figure 8. (**a**) Spatial positions of the strain change in the structure from stage III to stage VIII in vertical excavation. (**b**) Spatial positions of the strain change in the structure from stage III to stage X in lateral excavation.

3. Numerical Simulation

3.1. Finite Element Modeling

Abaqus is a powerful finite element software for engineering simulation, capable of solving a wide range of problems from relatively simple linear analysis to many complex nonlinear issues. It is widely used in the fields of underground engineering and foundation engineering [27,28]. This study used Abaqus finite element software to establish a three-dimensional finite element model, simulating the effects of vertical excavation and lateral excavation on the underground expansion project of the same existing building. The dimensions of the finite element model should be consistent with those of small-scale model tests. The model was proportionally reduced to a scale of 1:10.

The geometric dimensions of the upper structure, micropiles, diaphragm wall, and soil are the same as those of the experimental section. The structural model was divided into four layers, with main dimensions of 900 mm in length and 750 mm in width. The total height of the structure above the foundation was 1500 mm. The height of the first layer was 600 mm (including a 100 mm foundation embedment depth), and the heights of the second to fourth layers were 300 mm each. Additionally, the distance from the lateral boundary of the model and the distance from the lower bound of the model to the top were taken carefully so that the effects of the boundaries in the numerical model on the results were minimized. The displacement and the stress contours in the finite element software indicate that this distance is sufficient. In the excavation project, the size of the soil is usually selected as 40 times the diameter of the pile in order to minimize its impact on the results [29]. We decided to use soil simulating the excavation of a basement with dimensions of 1900 mm in length, 1900 mm in width, and 1400 mm in height. More information on the size of the model can be found in other published articles by our team [18,26].

The quality of grid division is closely related to the accuracy of finite element analysis. The more densely the finite element grid is divided, the higher the calculation accuracy, but the corresponding calculation cost will also increase. Therefore, in the process of grid division, we simulated the influence of different grid division precision on the results and found that the simulation results tend to stabilize when the number of grids reaches around 120,000. The change in the maximum stress value is not affected by the increase in the

number of grids. The grid independence analysis results are shown in Figure 9c. The final model grid total for the lateral excavation three-dimensional finite element model is 132,782, with a total of 149,158 nodes. The total number of grids for the vertical excavation three-dimensional finite element model is 113,902, with a total of 129,351 nodes. The boundary conditions, dimensions, relative positions, and grid division schematic diagram of the model are analyzed in Figure 9a,b.

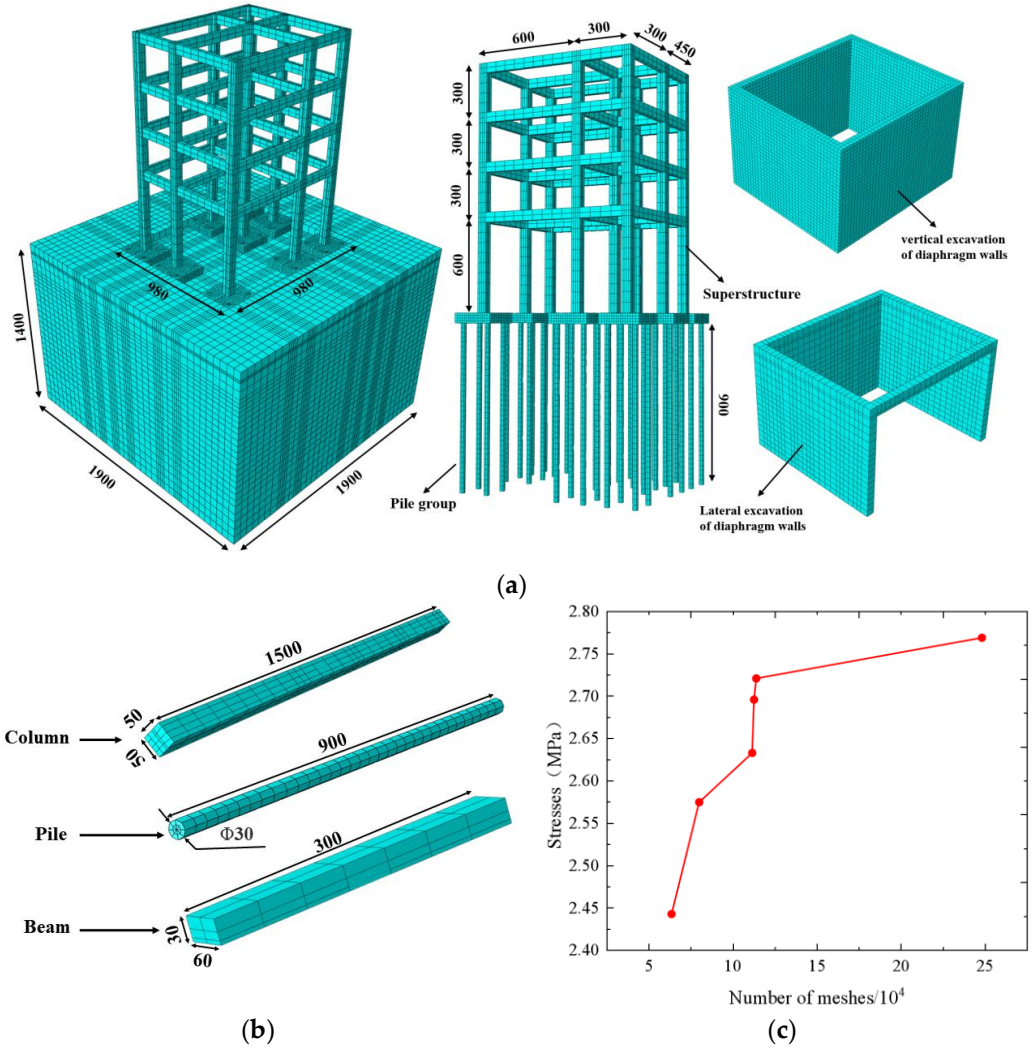

Figure 9. (**a**) Model dimensions and mesh diagram; (**b**) column, beam, pile dimensions, and grid diagram; (**c**) mesh sensitivity analysis.

This study assumes that soil is an ideal homogeneous elastic–plastic material to simulate the clay soil in Chengdu, and adopts the C3D8R three-dimensional eight-node finite element modeling, where "R" stands for the reduced integration method, which is less prone to self-locking under load [30]. According to previous studies, soil can be considered truly elastic within a very small range of strain, and its stiffness nonlinearly decreases as the strain amplitude increases [31]. Previous studies showed that the MC yield criterion had good adaptability and accuracy when the friction angle of soil was greater than 22°, and the DP failure criterion approached the MC yield criterion when the friction angle of soil was less than 22° [32]. The yield function and the plastic potential are shown in Formulas (4) and (5) [33].

$$f = p\sin\varphi + \sqrt{J_2\cos\theta} - \sqrt{\frac{J_2}{3}}\sin\varphi\sin\theta - C\cos\varphi \quad (1)$$

$$g = p\sin\Psi + \sqrt{J_2}\cos\theta - \sqrt{\frac{J_2}{3}}\sin\varphi\sin\theta - C\cos\varphi \quad (2)$$

where C, φ, and Ψ determine the cohesion, the friction angle, and the dilation angle of clay, respectively; p, J_2, and θ stand for the mean stress, the second invariant of the deviatoric stress tensor, and the Lode angle, respectively.

Another important reason for adopting this yield criterion is that only two strength parameters (cohesion and internal friction angle) are widely accepted and easily obtainable in practice, and the soil strength is determined by the inherent cohesion. Such studies can also be seen in the research of Lu et al. [34], who developed a nonlinear unified strength theory to construct a three-dimensional elastoplastic model using three independent material parameters. The friction angle (24.7°) and cohesion (20.1 kPa) were obtained from the soil tests conducted in the laboratory model tests, and the relevant supplementary information is elaborated in detail in other published articles by our team [18]. Additionally, the soil compression modulus was determined from the soil tests. In general, the elastic modulus is calculated based on the compression modulus at a ratio of 3 to 5 [35].

The stiffness of the structures, including the micropiles, superstructures, and retaining walls, is high, making it difficult to achieve plastic deformation. Therefore, a linear elastic model is adopted as the constitutive model. The material parameters of the linear elastic body are determined by Young's modulus and Poisson's ratio. The Young's modulus of the micropiles, superstructures, and retaining walls is calculated based on the standard value of concrete compressive strength measured through concrete compression tests using Formula (4) [36]. The parameters are fine-tuned according to the results of indoor experiments.

$$E_0 = 4700\sqrt{f_c'} \quad (3)$$

where f'_c is the standard compressive strength of the concrete facing.

Table 1 lists the material parameters required in finite element analysis.

Table 1. Material parameters used in finite element analysis.

Part	E (MPa)	C′ (kPa)	φ′ (°)	v	ρ (t^2/m^2)
Pile	2700	-	-	0.35	2.5
Upper_structure	30,000	-	-	0.35	2.5
Diaphragm wall	30,000	-	-	0.32	1.2
Soil	16.8	0	37	0.3	1.98

Regarding the constitutive model for contact surfaces, the interaction between the diaphragm wall and the soil, as well as the interaction between the piles and the soil is mainly the normal pressure exerted by the diaphragm wall on the soil and the tangential friction force. In this model, the contact surface is modeled using a "hard" contact model and a "penalty function" to simulate the interaction between the two. Under the "hard" contact model, when the pile is in close contact with the soil, the contact surface can transmit the normal force, and once the two are no longer in contact, the contact surface model will no longer transmit the force [37,38]. A penalty function based on Coulomb friction is used to simulate the tangential behavior of surface-to-surface contact. In this study, the effect of the diaphragm wall on the excavation of the basement is not considered because the interaction between the pile and the soil is the main cause of stress changes directly. The penalty function based on the Mohr–Coulomb model is shown in Equation (5) [39].

$$T = \mu\sigma_n \quad (4)$$

where T is the limiting shaft resistance of a pile, σ_n is the normal stress on the pile shaft, and μ is a frictional coefficient equal to 0.3.

The boundary conditions are as follows: the top of the model is a free constraint, the bottom is a fixed constraint, the left and right sides are constrained in the y direction. The

model is considered to be an axisymmetric model in the longitudinal direction, so the y-direction boundary condition is taken as an axisymmetric condition constraint, and the surface of the model is not restricted in the freedom of motion.

3.2. Numerical Modeling Procedure

The simulated excavation process consists of two methods: vertical excavation and lateral excavation. The difference in excavation procedures between the two excavation methods leads to differences in the lateral interaction between piles and soil, indirectly affecting the stress changes in the upper structure. This study compares and analyzes the effects of different excavation methods on structural stability and structural stress under the same existing structure. The simulation of the excavation process is reflected in the "interaction" part of Abaqus finite element software, which simulates the entire excavation process by killing modules and activating contacts [40]. Table 2 shows the excavation steps in vertical excavation method.

Table 2. Analysis steps of vertical excavation.

Step	Test Content
I	Initialize settings and balance the stresses of ground stress.
II	Balance the stress of micropiles, upper structures, and diaphragm walls.
III	Excavate the soil in III.
IV	Excavate the soil in IV.
V	Excavate the soil in V and VI.
VI	Excavate the top half of the soil beneath each single footing.
VII	Excavate the soil beneath each single footing.

The purpose of this study is to investigate the impact of the excavation process on structural stability, so the focus is on stages III~VII. Figure 10a,b is a supplement to the excavation steps. The specific state after the end of the eight different excavation steps is shown in Figure 11.

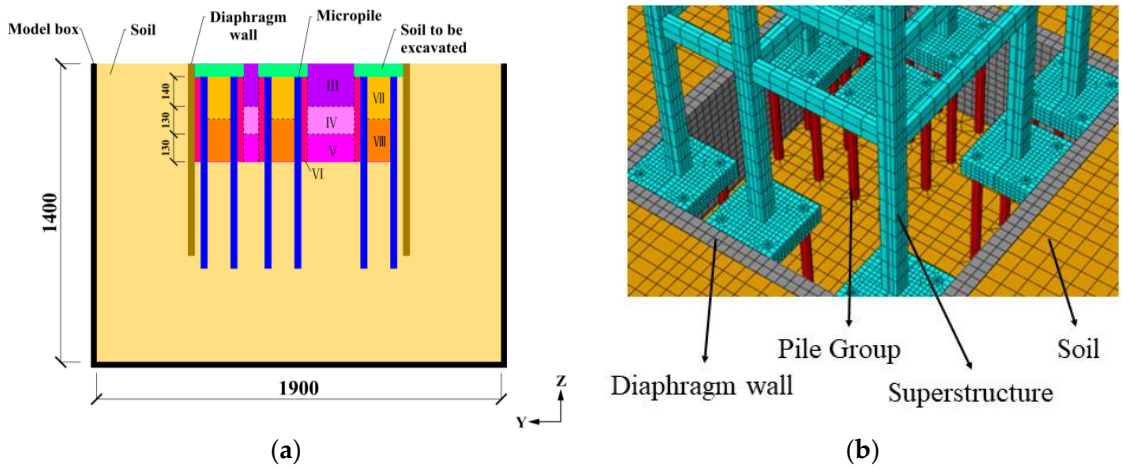

Figure 10. (**a**) Vertical excavation mode; (**b**) explanation of numerical simulation of vertical excavation.

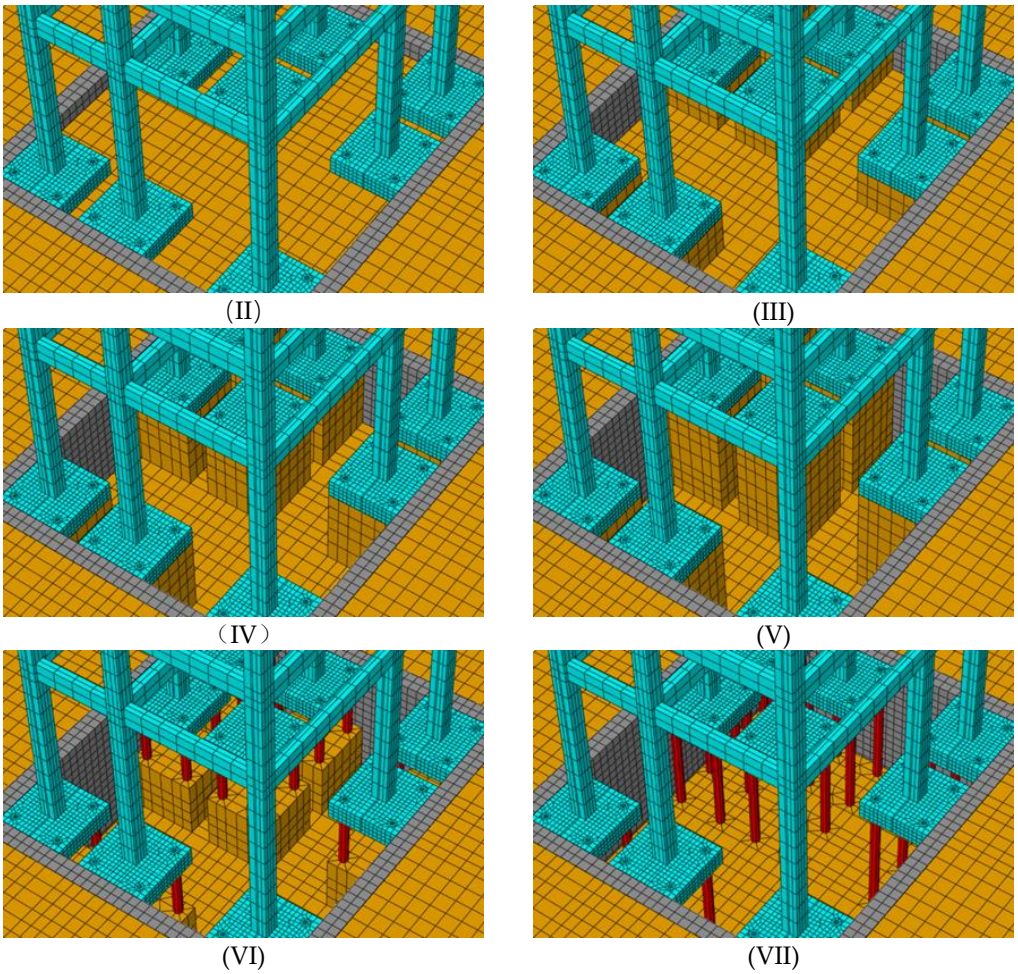

Figure 11. Numerical simulation of vertical excavation process. (note: II–VII represents excavation stage in Figure 3a).

Stepped slope excavation is lateral excavation. Compared to the former, the excavated soil is more complex, but the excavation depth and other related dimensions are the same as vertical excavation. The same method is adopted for balancing the ground stress in the early stage, as well as assembling the upper structure, pile foundation, and retaining wall. According to small-scale model experiments of underground space excavation, the calculation steps for vertical excavation of the three-dimensional finite element model are shown in Table 3 as follows.

Table 3. Analysis steps of lateral excavation.

Step	Test Content
I	Initialize settings and balance the stresses of ground stress.
II	Balance the stress of micro piles, upper structures, and diaphragm walls.
III	Excavate the soil in III.
IV	Excavate the soil in IV.
V	Excavate the soil in V.
VI	Excavate the soil in VI.
VII	Excavate the soil in VII.
VIII	Excavate the soil in VIII.
IX	Excavate the top half of the soil beneath each single footing.
X	Excavate the soil beneath each single footing.

As previously mentioned, the purpose of this study is to investigate the impact of excavation process on structural stability, so the focus is on stages III~X. The specific state after the end of the eight different excavation steps is shown in Figures 12 and 13.

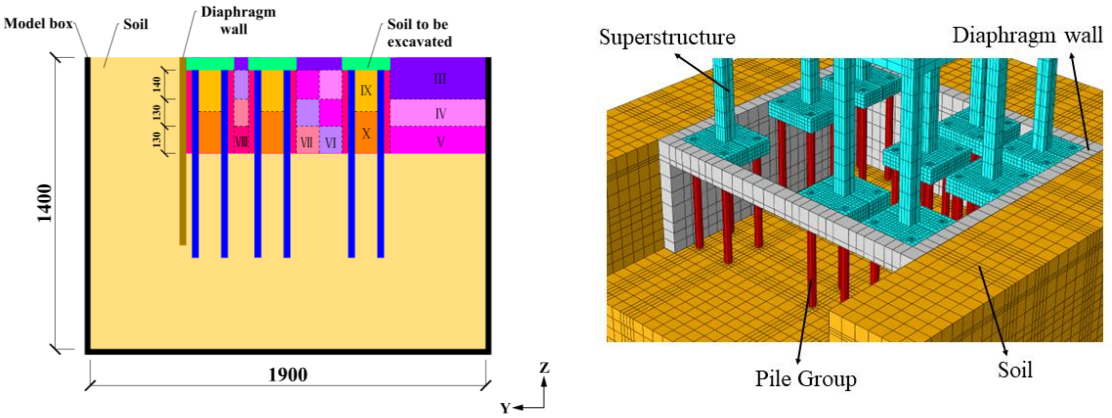

Figure 12. Explanation of numerical simulation of lateral excavation.

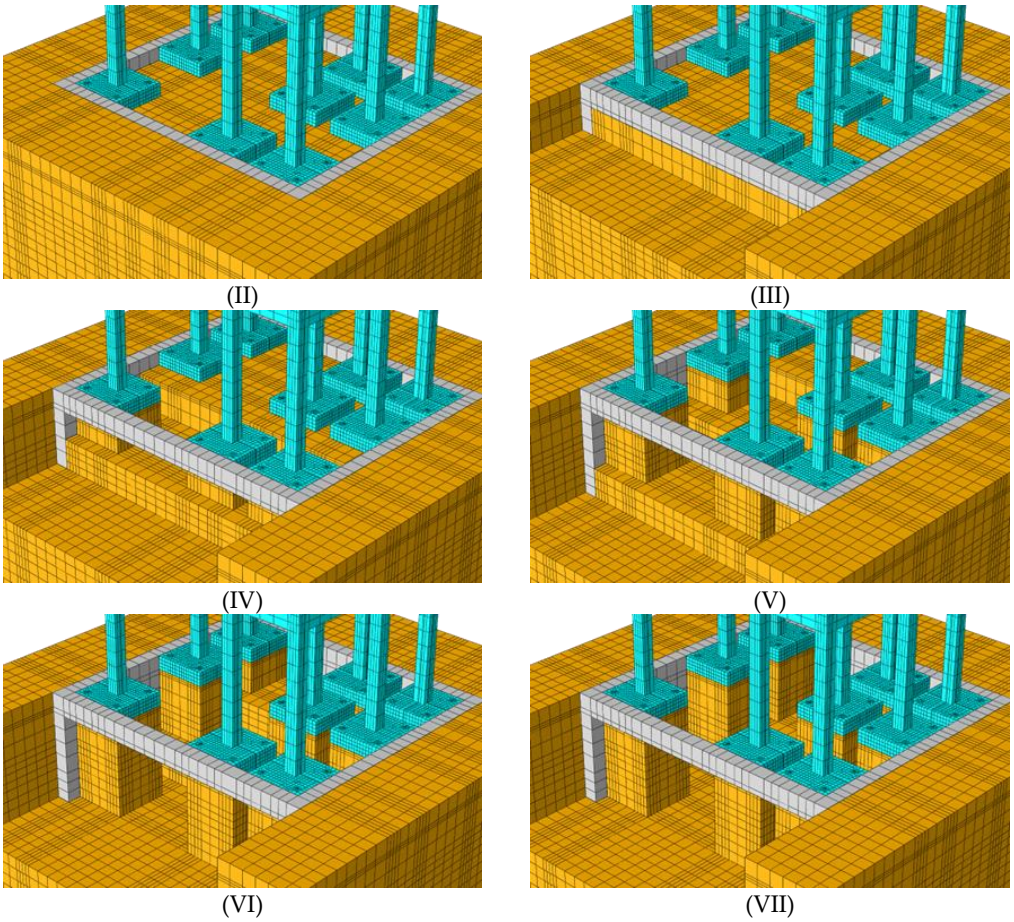

Figure 13. *Cont.*

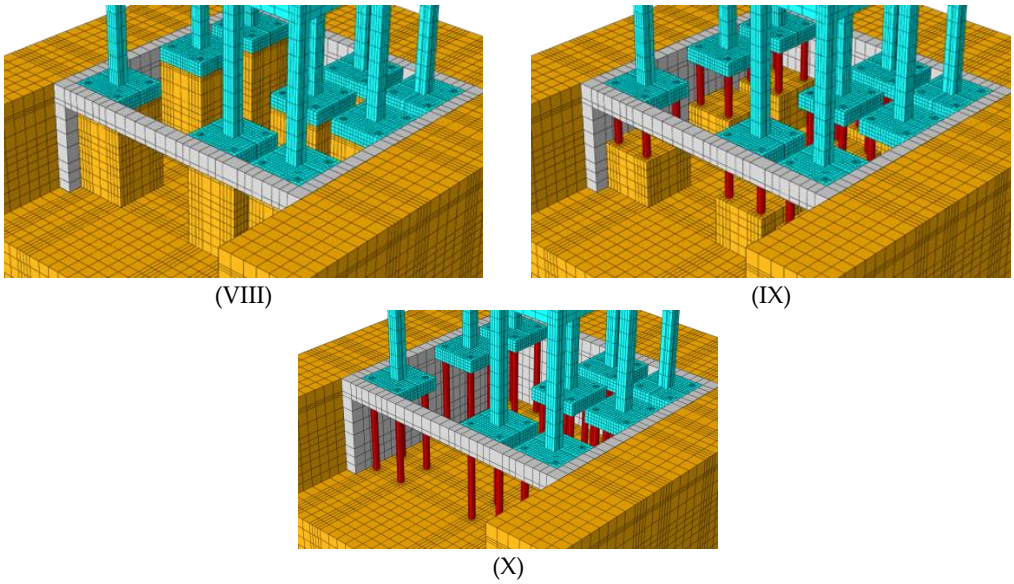

Figure 13. Finite element analysis during lateral excavation process. (note: II–X represents the excavation stage II–X in Figure 3a).

3.3. Finite Element Model Validation

We compared and analyzed the stress changes of the piles, beams, and columns obtained from numerical simulations, as well as the overall settlement of existing buildings in each stage to verify the rationality of the model. To increase the credibility of the experiment and reduce the workload of verification, this study randomly selected a set of stress data of the piles, beams, and columns from indoor model experiments and numerical simulations, as well as a set of settlement data for comparative analysis. It is important to highlight that in indoor model tests, strain gauges are used to measure strain changes at each point. However, it is not feasible to directly extract stress data for each monitoring point, thus, direct comparisons of their values cannot be made. Therefore, in verifying the stress changes of piles, beams, and columns, the focus is on the variation trend of each curve. In addition, in the following curves, L represents the result of the lateral excavation model, and V represents the result of vertical excavation.

Figure 14a,b shows the effects of vertical and lateral excavation on the existing structure column stresses in numerical simulations and indoor model tests, respectively. By analyzing the changes in the maximum stress of each layer of columns, the results indicate that with the advancement of the excavation stages, each excavation causes a small fluctuation in stress, and the stress of the columns gradually increases. At the same time, the experimental and numerical simulation results are consistent in the comparison of the peak stress values of the first and second layers of columns (i.e., the stress of the first layer is greater than that of the second layer).

In addition, in the indoor model test, the maximum strain values of the columns in vertical excavation and lateral excavation are 844 με and 7868 με, respectively. In numerical simulations, the maximum stress values of the columns during excavation and lateral excavation are 555 kPa and 655 kPa, respectively. The test and simulation results are consistent in terms of the response of columns to the two excavation methods. Lateral excavation has a greater impact on the stress of the columns in the existing structure above than vertical excavation.

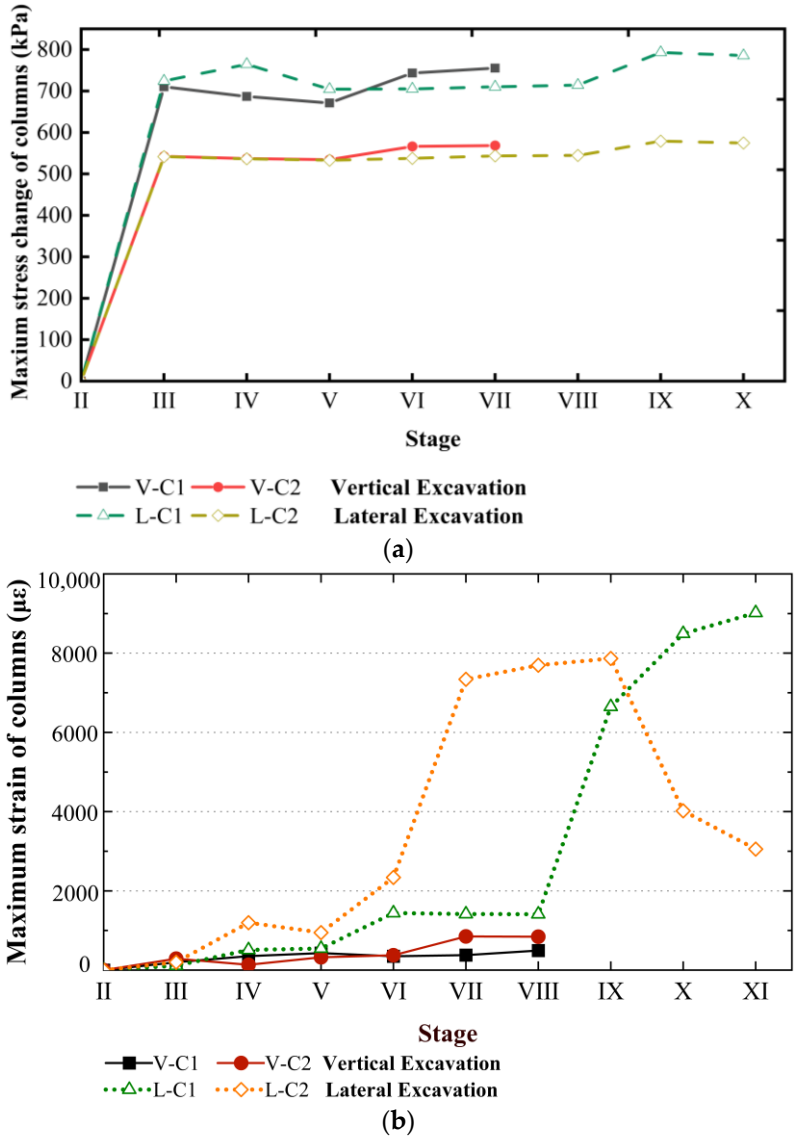

Figure 14. Maximum strain values of columns during vertical and lateral excavation: (**a**) Numerical simulation test structure; (**b**) indoor model test results.

Figure 15a,b shows the effects of vertical and lateral excavation on the existing structure beam stresses in numerical simulations and in-house model tests, respectively. By analyzing the changes in the maximum stress values of each layer of beams, it was found that the beam stresses gradually increased as the excavation stage progressed. Moreover, the results of the experimental and numerical simulations were consistent in the comparison of the peak stress values in the first and second columns (i.e., the first column had a greater peak stress than the second column).

In addition, different from the stress changes of the column, in the indoor model test, the maximum stress values of the beam excavated vertically and laterally were 6092 με and 6047 με, respectively. In numerical simulations, the maximum stress values of lateral excavation and vertical excavation are 393 kPa and 929 kPa, respectively. Both the experimental and simulation results indicate that vertical excavation has a greater impact on the stress of beams in the upper existing structure compared to lateral excavation. The specific reasons will be elaborated in detail in the stress analysis of the beam.

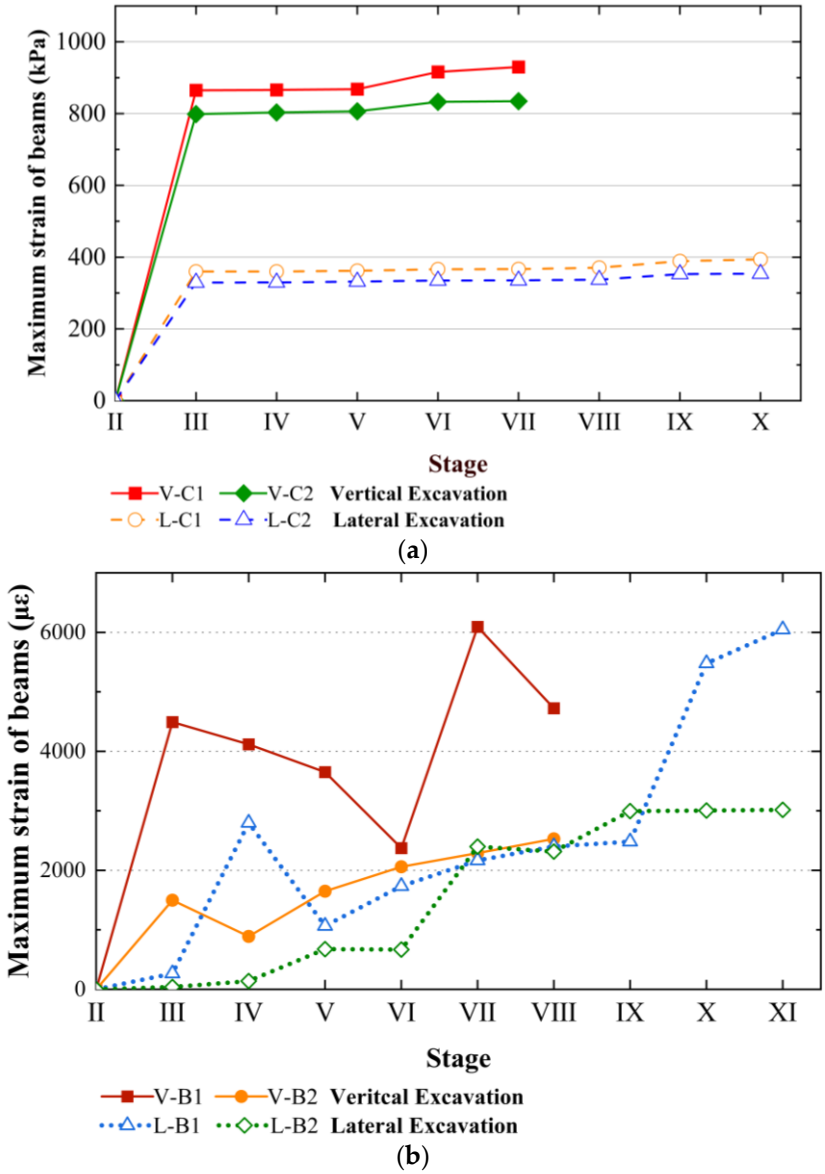

Figure 15. Maximum strain values of beams during vertical and lateral excavation: (**a**) Numerical simulation test structure; (**b**) indoor model test results.

Figure 16a,b shows the effects of vertical and horizontal excavation on the existing structure pile 4 in numerical simulations and indoor model tests, respectively. The numerical simulation results and the indoor test results show a good match in terms of trends, especially in the response of pile 4 to the excavation of the subgrade at the base of the abutment. As the excavation stage progresses, the internal force of pile 4 gradually increases. During the excavation process at the bottom of the pier cap, the stress of pile 4 rapidly increased in both the experiments and simulations. Moreover, in the two analysis methods, the stress values of column 4 in the vertical excavation model and the lateral excavation model are very similar, and both experiments and simulations show that the excavation method does not produce significant stress differences on the pile. The good agreement observed between the experiment and the model, both in terms of trend and final results, indirectly suggests that the two models are capable of accurately reflecting the stress changes of the supporting pile under various excavation conditions.

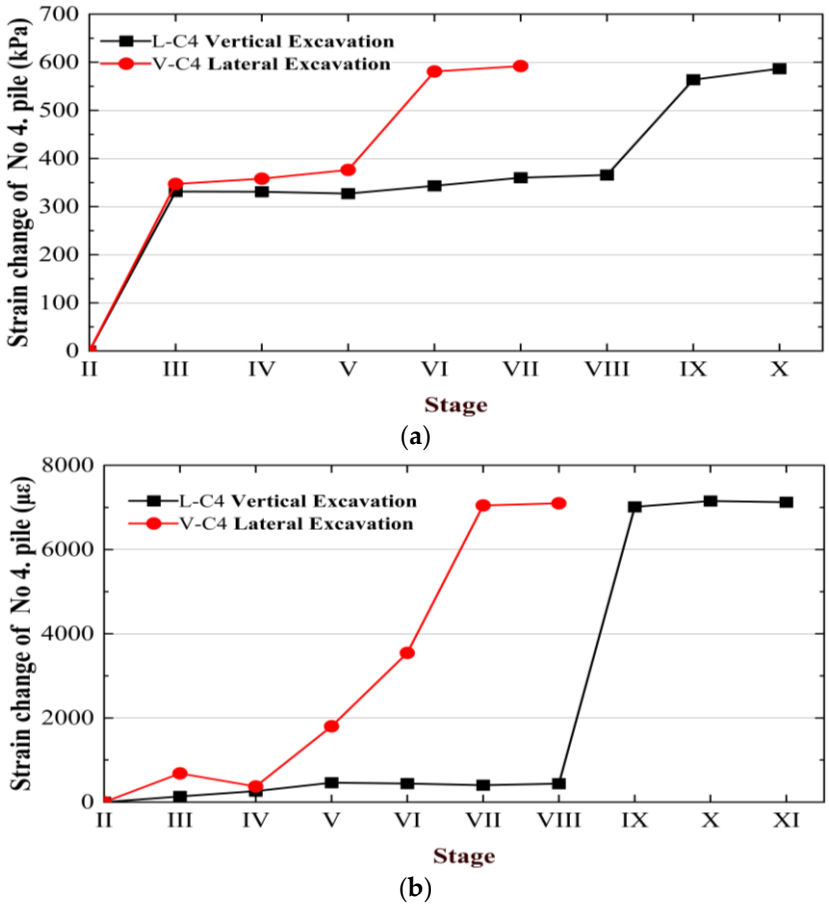

Figure 16. Maximum strain values of pile No. 4 during vertical and lateral excavation: (**a**) Numerical simulation test structure; (**b**) indoor model test results.

Figure 17a,b depicts the settlement results of vertical and lateral excavation of column 4 in the small-scale model experiments and finite element analysis. During the completion stage of excavation work, the settlement of column 4 increased to 0.11 mm and 0.24 mm, respectively, in the experimental and simulation results of the lateral excavation model. The maximum growth results of the vertical excavation model increased to 1.00 mm and 0.58 mm respectively, and the settlement values of both models showed an overall upward trend. At the same time, the settlement results of the two are not very different, and the degree of conformity is good.

We believe that the main reason for the differences in stress changes and building settlement increments of columns, beams, and piles, as well as the overall building deformation in each excavation stage between numerical simulations and in-house tests is that the basement heave phenomenon during the vertical excavation process is clearly visible in the in-house model tests, which is difficult to accurately simulate in finite element analysis. However, this study focuses on the comparative results of the impact of the two excavation methods on the existing building, and this kind of numerical error will not affect the subsequent analysis. Meanwhile, accurately simulating the basement heave phenomenon will be a key focus of future research.

Based on the analysis above, it can be inferred that the indoor model test and finite element simulation have good consistency in the stress changes of piles, beams, and columns, as well as the overall settlement results of existing buildings. This suggests that the experimental and calculated results align well with the general trend, confirming the feasibility of Abaqus simulation and the accuracy of both outcomes.

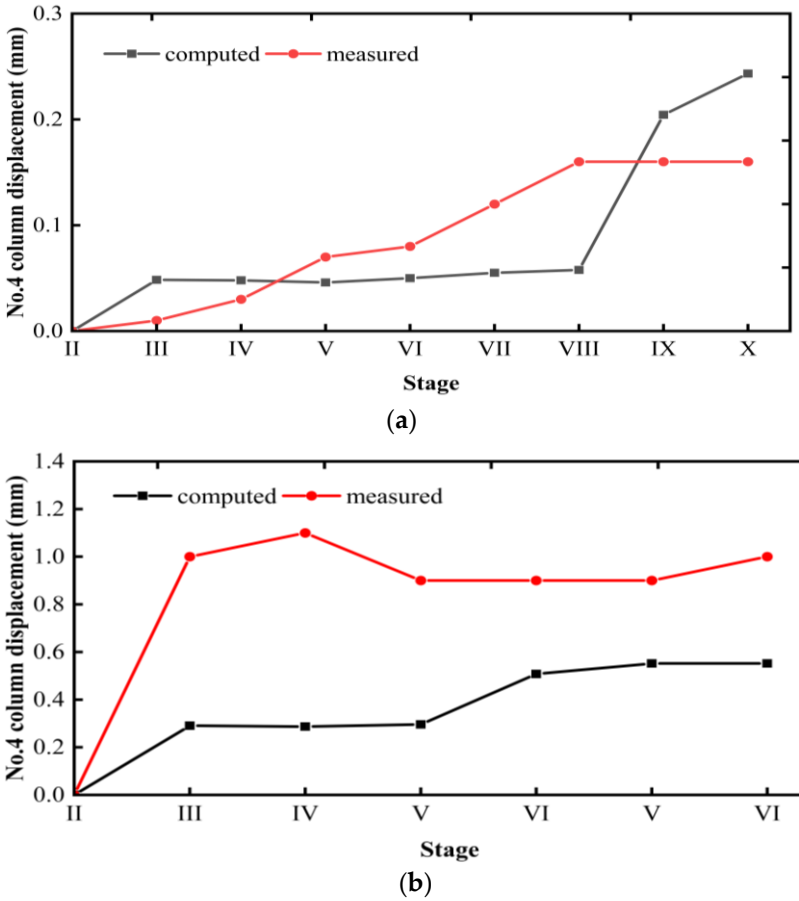

Figure 17. Vertical and lateral excavation settlement: (**a**) Numerical simulation test structure; (**b**) indoor model test results.

4. Result and Analysis

The process of buildings settling and the resulting stress changes in structures involve intricate transmission mechanisms. During the excavation process, the absence of soil will redistribute the stress field inside the pit, and the stress on the foundation soil will quickly transfer to the supporting piles. The stress variations in the piles can have an indirect impact on the stress conditions of the upper structure's beams and columns. This chain reaction will have adverse effects on the stability and structural load-bearing capacity of existing buildings.

In this section, we will conduct a comparative analysis of the outcomes obtained from the three-dimensional finite element simulation for lateral and vertical excavation and discuss the overall settlement of the building, as well as the stress changes of the piles, beams, and columns in order to comprehensively analyze the practical significance of lateral excavation and vertical excavation for underground layer expansion engineering.

4.1. Analysis of Underground Parts in Numerical Simulation

4.1.1. Overall Settlement of Existing Buildings

Figure 18 displays the settlement curves for each pile foundation in the lateral and vertical excavation methods.

The following can be determined from Figure 18:

(1) As excavation depth increases, the settlement of existing buildings experiences a notable increase. In the lateral excavation model, the maximum settlement increased from 0.05 mm in stage III to 0.24 mm in stage X. In the vertical excavation model, the maximum settlement of the columns increased from 0.29 mm in stage III to 0.58 mm in stage VII. In both the lateral and vertical excavation models, turning points were

observed in stages VIII and V (during excavation of the upper soil layer at the base of the bearing platform). These turning points, which represent the stress induced, may result from the swift transfer of foundation load to the supporting piles following the removal of soil around them.

(2) The maximum settlement value of the lateral excavation model column is 0.24 mm, while the maximum settlement value of the vertical excavation model column is 0.58 mm, which is approximately twice that of the lateral excavation model. The stability of the existing building is affected less by lateral excavation. This phenomenon may be due to the fact that the lateral excavation divides the soil into eight stages for excavation, while the vertical excavation only divides it into five stages. The construction cycle and the amount of soil excavated in each excavation method are different. Therefore, in cases where high stability is required, the vertical excavation method is more advantageous. At the same time, properly planning the amount of soil to be excavated and the construction cycle can effectively reduce the settlement impact of excavation on the existing building.

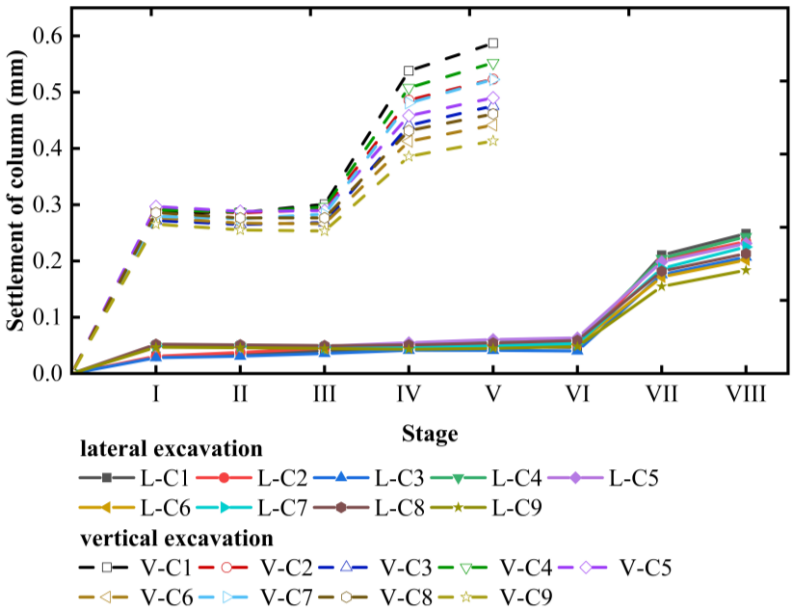

Figure 18. Settlement comparison chart.

4.1.2. Stress Variation of Piles

In the study, the average value of each point on a single pile is taken as the overall stress value of the pile. Figure 19a,b shows the stress variation curves of nine piles excavated laterally and vertically.

When analyzing the strain data of all the piles, the following can be seen:

(1) Overall, excavation caused strain fluctuations in the piles. As the excavation continues, the stress at each point on every pile demonstrates an increasing trend. In the lateral excavation model, the maximum pile stress increased from 362 kPa in stage III to 604 kPa in stage X. In the vertical excavation model, the maximum pile stress increases from 352 kPa in stage III to 602 kPa in stage VII. In stage VI of the lateral excavation model and stage IX of the vertical excavation model, there is a sharp increase in pile stress. This indicates that prior to excavating the soil beneath the bearing platform, the soil beneath the foundation is bearing the majority of the stress from the superstructure above. After the excavation of the soil at the bottom of the pier, the stress of the upper structure quickly transfers to the supporting piles.

(2) Comparing and analyzing the stress variation curves of lateral excavation and vertical excavation piles, it can be seen from the final results of the model and calculation that the maximum stress of the lateral excavation model and vertical excavation model

both occur at pile 1, with values of 604 kPa and 602 kPa, respectively. The maximum stress of the two is very similar. This indicates that different excavation methods do not cause significant stress differences in the support pile. Both excavation methods will cause significant stress fluctuations in the supporting pile. When excavating under existing buildings, regardless of the excavation method, the bearing capacity of the piles should be considered. If necessary, high-strength concrete materials should be used for the underpinning piles, and reinforcement should be reasonably arranged according to the actual situation to improve the strength of the supporting piles. At the same time, the soil at the bottom of the bearing platform should be divided into smaller soil blocks to prevent the rapid transfer of stress during the excavation process of this part of the soil, which may cause damage to the supporting piles.

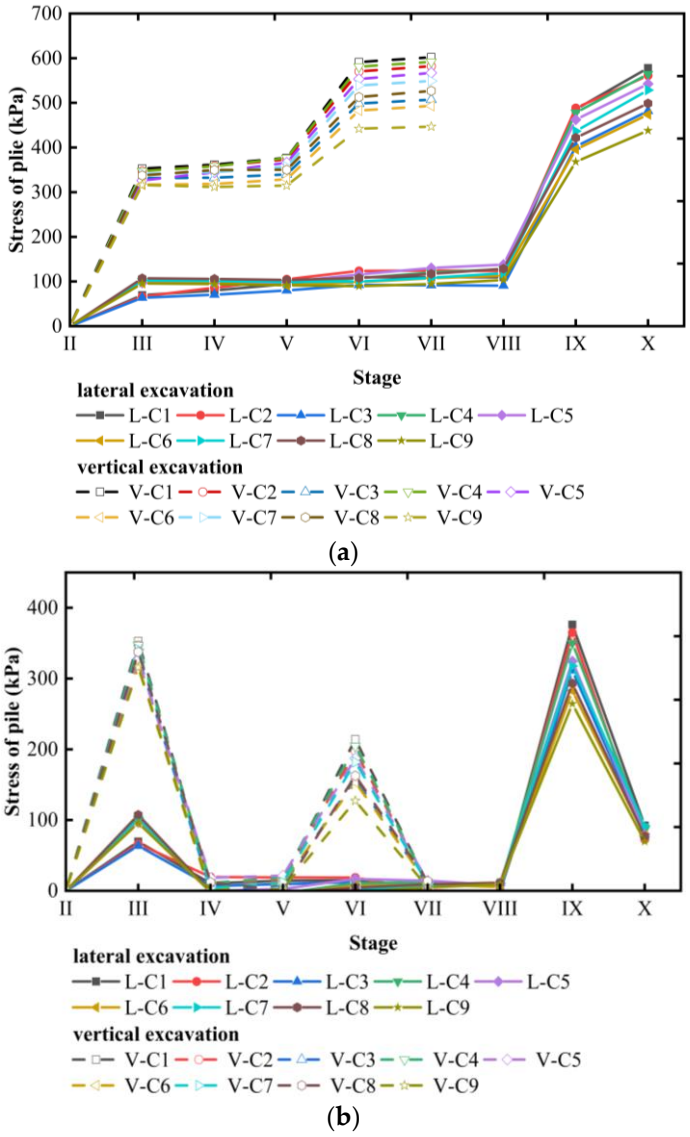

Figure 19. (**a**) Stress curves of 9 piles during lateral excavation; (**b**) stress curves for vertical excavation of 9 piles.

4.2. Analysis of Aboveground Parts in Numerical Simulation

4.2.1. Stress Changes in Columns

Figure 20 shows the stress changes of the second layer column under two different excavation methods.

(1) As the excavation stage progresses, the stress in the columns gradually increases. In the lateral excavation model, the maximum stress increased to 815 kPa; in the vertical excavation model, the maximum stress increased to 745 kPa. Lateral excavation will cause greater stress fluctuations in the upper structure columns, and vertical excavation will be a better choice for existing building renovation projects with weaker column strength in the upper structure.

(2) The stress changes during the excavation of the columns are unpredictable. Therefore, real-time monitoring of the stress changes in the upper structure is needed during construction, and support should be provided for areas with high stress to alleviate the unfavorable stress state of the structure. At the same time, when the structure's stress deteriorates, the excavation volume for the next stage should be reduced and the construction progress slowed down. When the structure's stress changes are not significant, consideration should be given to increasing the excavation volume for the next stage appropriately.

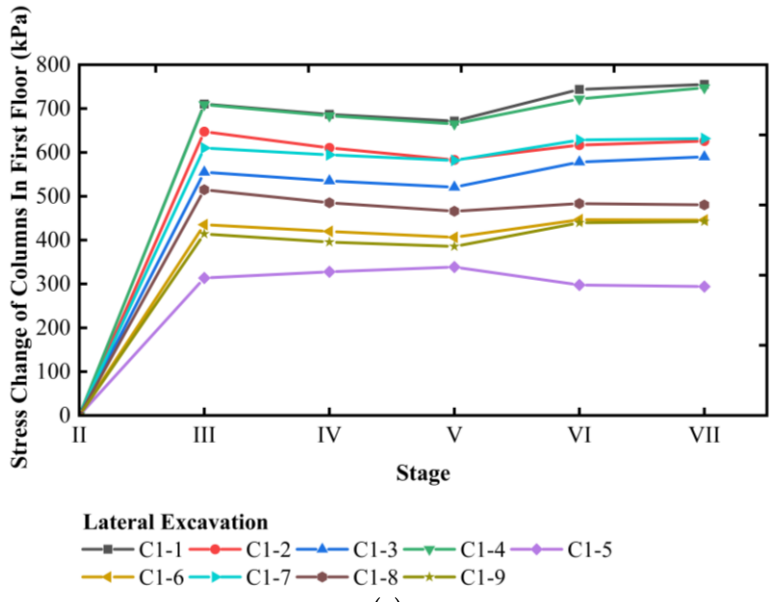

(**a**)

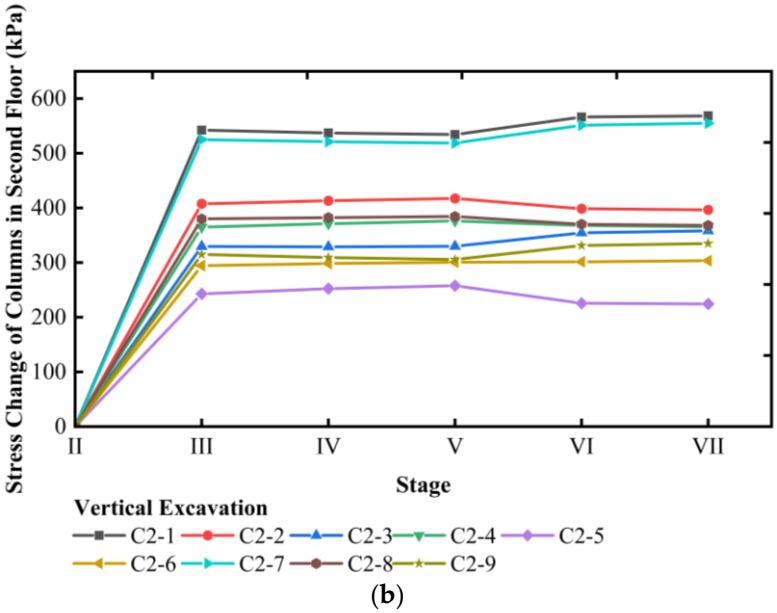

(**b**)

Figure 20. *Cont.*

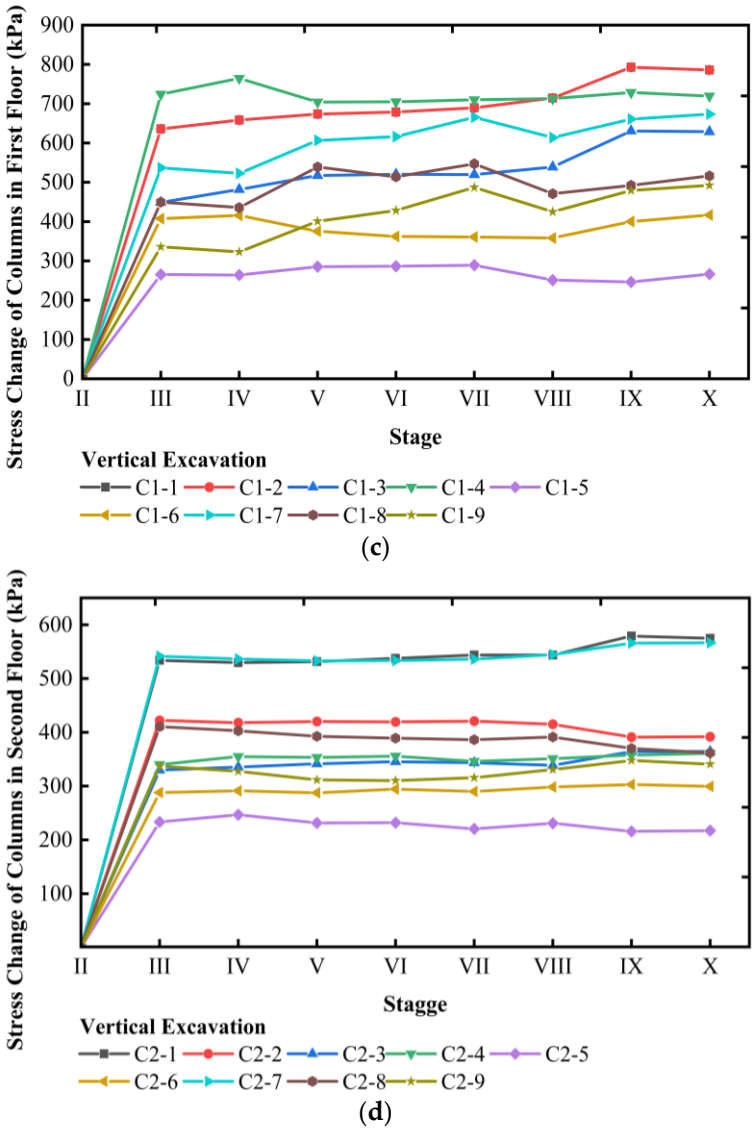

Figure 20. (**a**) Stress variation diagram of the first-layer column during vertical excavation; (**b**) vertical first-layer column stress variation diagram; (**c**) stress comparison diagram of the first-layer column during lateral excavation; (**d**) stress comparison diagram of the second-layer column during lateral excavation.

4.2.2. Stress Changes in Beams

Figure 21a,b depicts the stress variation comparison curves of the first- and second-layer beams under different excavation methods.

By comparing and analyzing the calculation results of the lateral excavation model and the vertical excavation model, the following rules are obtained:

(1) The stress changes of the beams show an overall upward trend. Each excavation causes fluctuations in the beam stress, but the stress fluctuations in each stage are relatively small. There is a significant difference in the maximum stress values that the beams bear under lateral and vertical excavation. The maximum stress values that the beams bear under vertical excavation are about 2–3 times those under lateral excavation. Among them, the maximum stress value of the first-layer beam in the lateral excavation model is 393.831 kPa, and the maximum stress value of the second-layer beam is 353.856 kPa. In the vertical excavation model, the maximum stress value of the first-layer beam is 930 kPa, and the maximum stress value of the second-layer beam is 834.573 kPa. The influence of vertical excavation on the existing

structure beams is much greater than that of lateral excavation. In existing building renovation projects with weak upper-structure beams, lateral excavation will be a more suitable choice.

(2) When choosing the lateral excavation method, it is particularly important to provide adequate support or reinforcement for beams with potential stress changes, especially the first-layer beams and the areas where the stress is greater, such as the connections between the beams and columns. At the same time, real-time monitoring can also effectively mitigate the impact of excavation on beams, just like the columns.

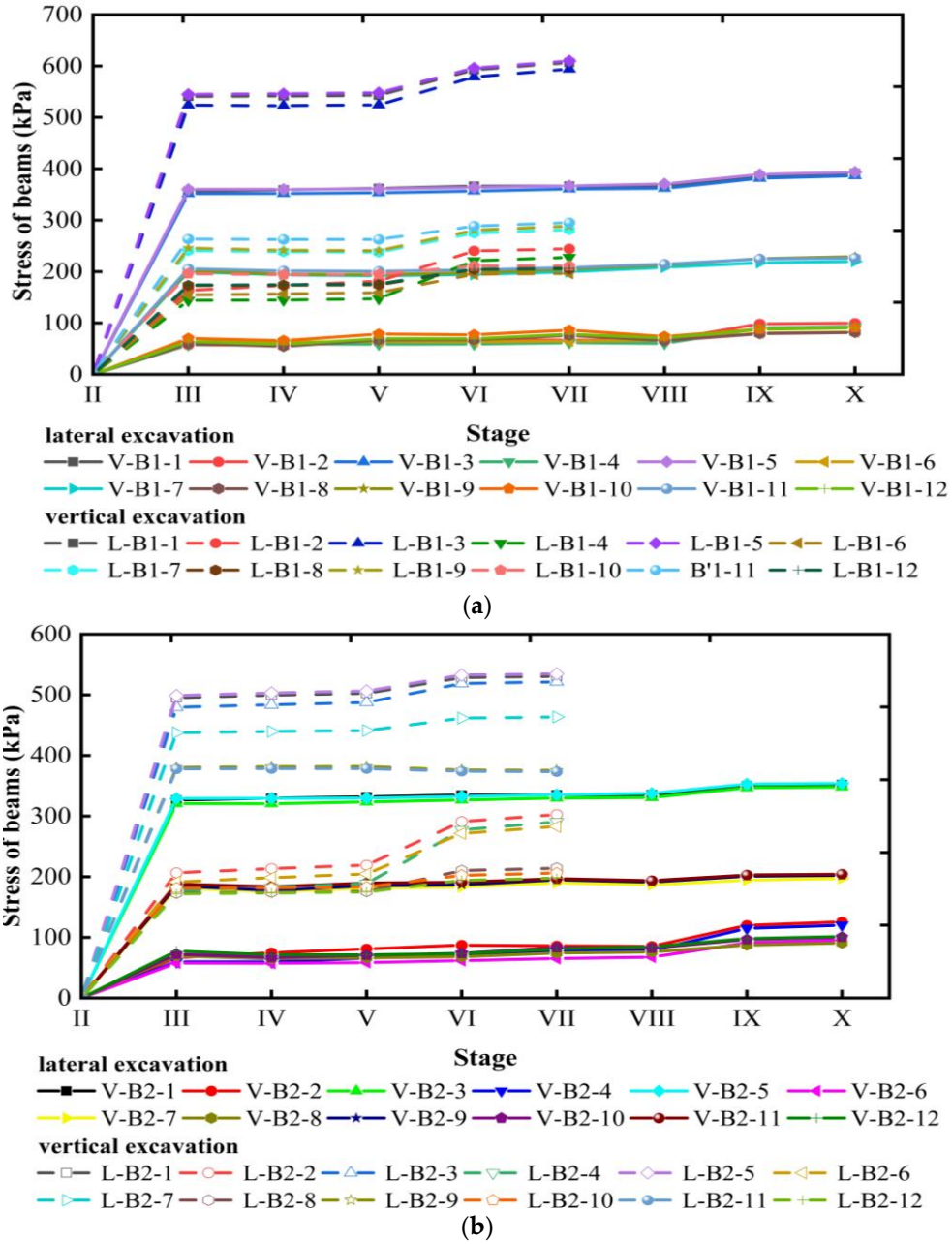

Figure 21. Stress variation diagram of lateral excavation and vertical excavation beams: (**a**) Comparison diagram of stress in the first-layer beam; (**b**) comparison diagram of stress changes in the second-layer beam.

4.3. Stress Analysis at Structural Spatial Positions

Figure 22 shows the von Mise stress cloud map results of vertical excavation and lateral excavation simulated by Abaqus finite element software at each stage. From the analysis

above, it can be seen that the stress changes in the upper structure during excavation are not significant, while the piles will have significant stress fluctuations. Therefore, when extracting the stress cloud map, we separately extract the pile and adjust its stress threshold to make its changes more pronounced.

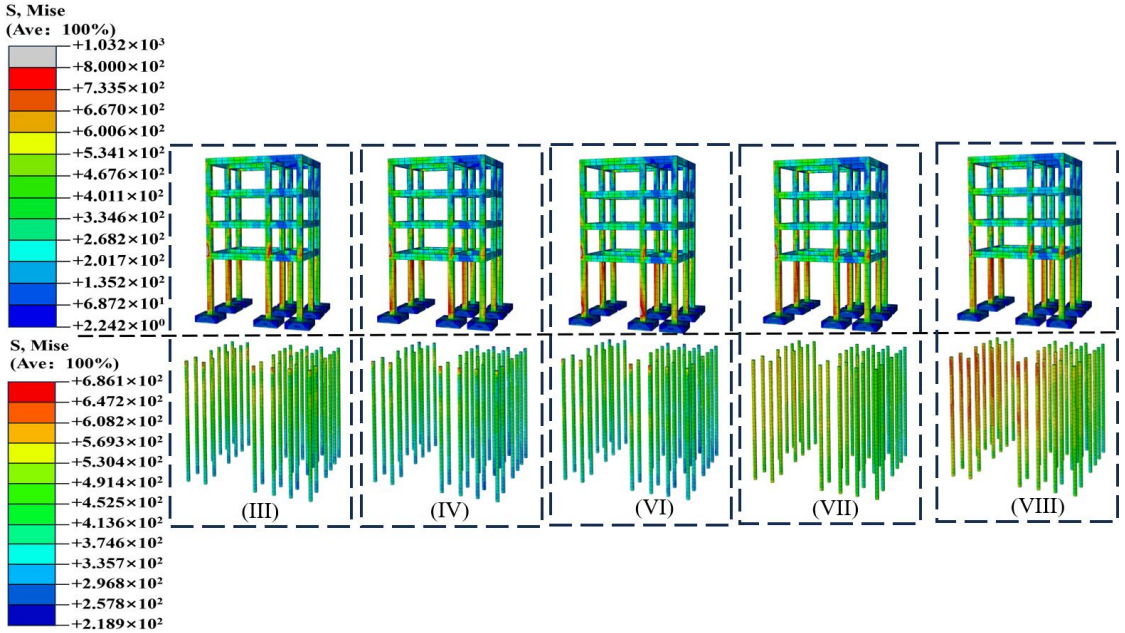

(**a**)

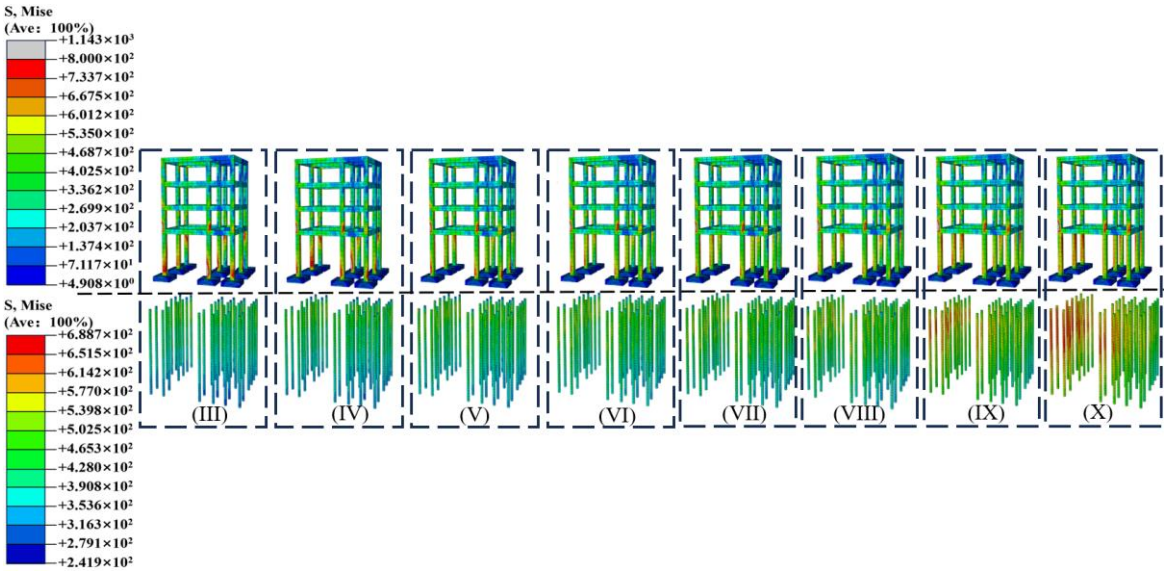

(**b**)

Figure 22. (**a**) Von Mise stress cloud map of upper structure and pile foundation in each stage of vertical excavation; (**b**) von Mise stress cloud map of upper structure and pile foundation in each stage of lateral excavation.

The force conditions of each component are similar to the patterns obtained from indoor model tests, as follows:

(1) In the two different excavation methods, the strain values of different structural components will be different. Generally speaking, the internal forces of the structure from high to low are columns, piles, and beams in both excavation methods, but compared with vertical excavation, lateral excavation will produce greater column stresses and more dramatic changes in pile stresses. The stress of beams and the

overall settlement of the building are more responsive to the vertical excavation method. This difference may be caused by the uneven distribution of internal forces in different excavation conditions or the difference in excavation cycle and excavation volume. Therefore, in actual engineering projects, the appropriate excavation method should be selected according to the structural features of the building.

(2) From the three-dimensional Mise stress cloud map of transverse and vertical excavation, it can be seen that the stress is mainly generated at the top of the pile end, the first layer of the superstructure, and the structural joints during excavation. When excavation is carried out, the structure needs to be monitored in real time, and temporary support or reinforcement measures are provided for areas with large changes in stress. At the same time, it is very important to adjust the construction schedule according to the real-time monitoring data, especially considering the possibility of uneven settlement in the later stages of construction, resulting in stress peaks in stages VII and X. Appropriate reduction of construction progress and earthwork volume can effectively reduce the adverse stress state of the structure.

5. Conclusions and Future Prospects

Based on the numerical simulation method, this study analyzes the effects of lateral and vertical excavation methods on the stress changes and settlement values of piles, columns, and beams of existing buildings. The following conclusions can be drawn:

(1) This paper proposes a numerical simulation method based on the modification of experimental model parameters to analyze the effects of different excavation conditions on the stability of existing buildings. In the process of debugging model parameters, the team iterates the three-dimensional finite element model according to material parameters and model test results, so that the numerical simulation results and indoor model test results maintain good consistency in the stress changes and settlement changes of piles, beams, and columns. The test results and simulation results show that with the progress of the excavation stage, the stress values of piles, columns, and beams gradually increase due to the excavation of the soil. In addition, under the two excavation methods, the stress fluctuations of columns and beams at each stage are not large. On the contrary, the stress changes of the pile foundation are very obvious, especially in the excavation of the soil under the bearing plate. The disappearance of the soil around the pile will lead to the rapid transfer of the upper load originally carried by the foundation soil to the pile, which will have an adverse effect on it.

(2) In both excavation methods, the internal forces of the structure are in the order of columns, piles, and beams. However, compared to vertical excavation, lateral excavation will result in larger column stresses and more dramatic pile stress increments. Vertical excavation, on the other hand, will increase the beam stress and building settlement value. The characteristic of excavating from one side will cause the structure to lean towards the excavation side, which is one of the reasons why the columns and piles on the excavation side produce larger stresses. Vertical excavation will cause the central columns to experience larger settlement, which leads to the beams bearing larger stresses to resist uneven settlement. It is particularly important to choose a reasonable excavation method based on the characteristics of the building structure and the site conditions. In areas with soft soil and weak foundation bearing capacity, lateral excavation, which has a smaller impact on the settlement of existing buildings, will be a better choice for underground excavation. When excavating soil under an aging upper structure, vertical excavation, which has a smaller impact on the stress changes of the upper structure, will be the preferred option.

(3) Both excavation methods will result in significant induced stresses at the lower part of the structure, the upper part of the pile foundation, and the connection between the structure and foundation. By analyzing the three-dimensional spatial stress distribution of the two numerical simulation models, it can be seen that the stress values at the upper and lower parts of the existing building's pile foundation are

relatively high. At the same time, the stress at the connection between the pile cap and pile and the column–beam joint may also be significant. Therefore, in subsequent research, it is necessary to pay attention to these stress changes and optimize the structural reinforcement and foundation reinforcement schemes.

(4) By summarizing and analyzing the test and numerical simulation results, we have proposed some engineering suggestions that may be helpful in the future. The excavation cycle and excavation volume are important factors affecting structural stability. When the structural stress deteriorates, the excavation volume for the next stage should be reduced or the excavation cycle should be extended. When the structural stress changes little, the excavation volume for the next stage can be increased or the excavation cycle can be shortened. At the same time, reasonable reinforcement and support methods can effectively alleviate the generation of structural induced stresses. Before excavation, the permanent reinforcement of the nodes with stress changes that are large should be carried out based on the theoretical analysis and numerical simulation results. During excavation, temporary support should be provided for the newly generated nodes with stress changes that are large to ensure the structural stability during the construction process. After excavation, the temporary support components should be removed, and the nodes with stress that have not dissipated should be reinforced permanently.

Author Contributions: Writing—original draft, software, J.T.; methodology, Z.W.; supervision, funding acquisition, Y.M.; writing—review & editing, resources, H.Z.; dada curation, Y.H.; investigation, R.L.; validation, P.T. All authors have read and agreed to the published version of the manuscript.

Funding: This research was funded by Yunnan Fundamental Research Projects (No. 202301AT070386) and the Talent Development Fund of Kunming University of Science and Technology (No. KKZ3202306032).

Data Availability Statement: The data used to support the findings of this study are available from the corresponding author upon request.

Acknowledgments: The authors are grateful to the financial support from Kunming University of Science and Technology.

Conflicts of Interest: Author Peigen Tang was employed by the Baihetan Hydropower Plant, China Yangtze Power Co., Ltd., Ningnan 615400, China. The remaining authors declare that the research was conducted in the absence of any commercial or financial relationships that could be construed as a potential conflict of interest.

References

1. Fu, C.; Deng, T.; Zhang, Y. Boosted efficiency and unsaturated material stock growth in China's megacities: Accelerating as urbanization approaches 80%. *Resour. Conserv. Recycl.* **2024**, *203*, 107417. [CrossRef]
2. Schiller, G.; Roscher, J. Impact of urbanization on construction material consumption: A global analysis. *J. Ind. Ecol.* **2023**, *27*, 1021–1036. [CrossRef]
3. Shahraki, A.A. Renovation programs in old and inefficient neighborhoods of cities with case studies. *City Territ. Archit.* **2022**, *9*, 28. [CrossRef]
4. Lihtmaa, L.; Kalamees, T. Emerging renovation strategies and technical solutions for mass-construction of residential districts built after World War II in Europe. *Energy Strategy Rev.* **2024**, *51*, 101282. [CrossRef]
5. Zhao, T.; Gao, Y.; Zhan, W.; Sun, H.; Zhang, T.; Li, L.; Zuo, W.; Tang, X.; Li, Y.; Tian, Y. Municipal solid waste (MSW) under the population shrinking and aging: Spatio-temporal patterns, driving forces, and the impact of smart city development. *J. Clean. Prod.* **2024**, *434*, 140124. [CrossRef]
6. Zhang, X.-l.; Jun-yuan, X.; Cheng-shun, X.; Kai-yuan, L. An analysis method for lateral capacity of pile foundation under existing vertical loads. *Soil Dyn. Earthq. Eng.* **2021**, *142*, 106547. [CrossRef]
7. Pei, H.R. Research on foundation stability of building based on foundation bearing capacity. *Appl. Mech. Mater.* **2014**, *624*, 661–664. [CrossRef]
8. Fan, H.; Xu, Q.; Lai, J.; Liu, T.; Zhu, Z.; Zhu, Y.; Gao, X. Stability of the loess tunnel foundation reinforced by jet grouting piles and the influence of reinforcement parameters. *Transp. Geotech.* **2023**, *40*, 100965. [CrossRef]
9. Gkournelos, P.; Triantafillou, T.; Bournas, D. Seismic upgrading of existing reinforced concrete buildings: A state-of-the-art review. *Eng. Struct.* **2021**, *240*, 112273. [CrossRef]

10. Zhou, Z.; Zhou, Y.; Zhang, H.; Chen, S.; Xiang, L.; Wang, L. Effects of Foundation Excavation on Metro Tunnels at Different Locations and Performance of Corresponding Reinforcement Measures: A Case of Shenzhen Metro Line 11, China. *Symmetry* **2022**, *14*, 2561. [CrossRef]
11. Park, Y.-H.; Kim, J.-P.; Cho, K.-H. Stability analysis of subway box structure supported by modified underpinning method. *Tunn. Undergr. Space Technol.* **2015**, *50*, 199–208. [CrossRef]
12. Bovolenta, R.; Brencich, A. Effect of deep excavations and deformable retaining structures on neighboring buildings: A case study. *Eng. Fail. Anal.* **2021**, *122*, 105269. [CrossRef]
13. Dmochowski, G.; Szolomicki, J. Technical and Structural Problems Related to the Interaction between a Deep Excavation and Adjacent Existing Buildings. *Appl. Sci.* **2021**, *11*, 481. [CrossRef]
14. Fan, X.; Xu, C.; Liang, L.; Yang, K.; Chen, Q.; Feng, G.; Zhang, J. Experimental and Numerical Study of Braced Retaining Piles with Asymmetrical Excavation. *Int. J. Civ. Eng.* **2024**, *22*, 1339–1356. [CrossRef]
15. Gang, Z.; Yu-ping, W.; Xue-song, C.; Di-hua, Y.; Peng, Z.; Wen-long, C.; Yue-bin, Z.; Xin-hao, L. Large-scale model tests on performance and mechanism of inclined retaining structures of excavations. *Chin. J. Geotech. Eng.* **2021**, *43*, 1581–1591. [CrossRef]
16. Yu, S.; Geng, Y. Influence Analysis of Underground Excavation on the Adjacent Buildings and Surrounding Soil Based on Scale Model Test. *Adv. Civ. Eng.* **2019**, *2019*, 6527175. [CrossRef]
17. Zhang, X.; Wang, S.; Liu, H.; Cui, J.; Liu, C.; Meng, X. Assessing the impact of inertial load on the buckling behavior of piles with large slenderness ratios in liquefiable deposits. *Soil Dyn. Earthq. Eng.* **2024**, *176*, 108322. [CrossRef]
18. Miao, Y.; Liu, B.; Liu, C.; Shu, Z.; Wu, H. Experimental Study on Stability Analysis of a Structure during Excavation beneath This Structure. *Adv. Civ. Eng.* **2020**, *2020*, 9268927. [CrossRef]
19. Chheng, C.; Likitlersuang, S. Underground excavation behaviour in Bangkok using three-dimensional finite element method. *Comput. Geotech.* **2018**, *95*, 68–81. [CrossRef]
20. Li, Z.; Chen, Z.; Wang, L.; Zeng, Z.; Gu, D. Numerical simulation and analysis of the pile underpinning technology used in shield tunnel crossings on bridge pile foundations. *Undergr. Space* **2021**, *6*, 396–408. [CrossRef]
21. Lou, P.; Huang, W.; Huang, X. Analysis of Shield Tunnels Undercrossing an Existing Building and Tunnel Reinforcement Measures. *Appl. Sci.* **2023**, *13*, 5729. [CrossRef]
22. Xue, H. Research on the Control of Excavation Deformation of Super Deep Foundation Pit Adjacent to the Existing Old Masonry Structure Building. *Sustainability* **2023**, *15*, 7697. [CrossRef]
23. Li, H.; Liu, S.; Tong, L. A numerical interpretation of the soil-pile interaction for the pile adjacent to an excavation in clay. *Tunn. Undergr. Space Technol.* **2022**, *121*, 104344. [CrossRef]
24. Shan, H.-F.; He, S.-F.; Lu, Y.-H.; Jiang, W.-J. Case Study and Numerical Simulation of Excavation beneath Existing Buildings. *Adv. Civ. Eng.* **2020**, *2020*, 8817339. [CrossRef]
25. Harrington, P.F.; Reip, D.W. Design for Underpinning the Central Artery. In *Restructuring: America and beyond*; ASCE: Reston, VA, USA, 1995; pp. 867–881.
26. Miao, Y.; Liu, B.; Liu, C.; Shu, Z.; Wu, H. Experimental Study on the Displacement and Strain of Underpinning Piles during Basement Excavation. *Soil Mech. Found. Eng.* **2022**, *59*, 141–147. [CrossRef]
27. Zamora Hernández, Y.; Durand Farfán, A.; Pacheco de Assis, A. Three-dimensional analysis of excavation face stability of shallow tunnels. *Tunn. Undergr. Space Technol.* **2019**, *92*, 103062. [CrossRef]
28. Liu, K.; Chen, S.L.; Gu, X.Q. Analytical and Numerical Analyses of Tunnel Excavation Problem Using an Extended Drucker–Prager Model. *Rock Mech. Rock Eng.* **2020**, *53*, 1777–1790. [CrossRef]
29. Yuanyuan, J.; Fu, L.J.; Ran, Z.; Huiying, W. Load bearing capacity of the large-diameter steel pipe piles under vertical loads. *J. Guangxi Univ. (Nat. Sci. Ed.)* **2012**, *37*, 744–750. [CrossRef]
30. He, S.; Lai, J.; Li, Y.; Wang, K.; Wang, L.; Zhang, W. Pile group response induced by adjacent shield tunnelling in clay: Scale model test and numerical simulation. *Tunn. Undergr. Space Technol.* **2022**, *120*, 104039. [CrossRef]
31. Atkinson, J. Experimental determination of stress-strain-time characteristics in laboratory and-in-situ tests. General report. In Proceedings of the 10th European Conference on Soil Mechanics and Foundation Engineering, Florence, Italy, 26–30 May 1991; pp. 915–956.
32. Xiang-Rong, Z.; Jin-Chang, W. Introduction to partly soil models in ABAQUS Software and their application to the geotechnical engineering. *Rock Soil Mech.* **2004**, *25*, 145–148.
33. Mroueh, H.; Shahrour, I. Three-dimensional finite element analysis of the interaction between tunneling and pile foundations. *Int. J. Numer. Anal. Methods Geomech.* **2002**, *26*, 217–230. [CrossRef]
34. Lu, D.; Ma, C.; Du, X.; Jin, L.; Gong, Q. Development of a New Nonlinear Unified Strength Theory for Geomaterials Based on the Characteristic Stress Concept. *Int. J. Geomech.* **2017**, *17*, 04016058. [CrossRef]
35. Zhongxiang, C.; Shannan, L.; Chengyong, G.; Shengnan, H. Analysis of Lateral Response of Bored Piles Based Onconcrete Damaged Plasticity Model. *Chin. J. Rock Mech. Eng.* **2014**, *33*, 4032–4040. [CrossRef]
36. Maleki, M.; Khezri, A.; Nosrati, M.; Hosseini, S.M.M.M. Seismic amplification factor and dynamic response of soil-nailed walls. *Model. Earth Syst. Environ.* **2023**, *9*, 1181–1198. [CrossRef]
37. Tengyue, Z.; Sheng, L.; Jie, H.; Chen, Z.; Haiding, B.; Weiwei, Y. Analysis of Lateral Deformation of Adjacent Pile Foundation in Foundation Excavation. *Constr. Technol.* **2022**, *51*, 40–45.

38. Zhan, Y.; Wang, H.; Liu, F. Modeling vertical bearing capacity of pile foundation by using ABAQUS. *Electron. J. Geotech. Eng.* **2012**, *17*, 1855–1865.
39. Soomro, M.A.; Hong, Y.; Ng, C.W.W.; Lu, H.; Peng, S. Load transfer mechanism in pile group due to single tunnel advancement in stiff clay. *Tunn. Undergr. Space Technol.* **2015**, *45*, 63–72. [CrossRef]
40. Liu, C.; Cui, J.; Zhang, Z.; Liu, H.; Huang, X.; Zhang, C. The role of TBM asymmetric tail-grouting on surface settlement in coarse-grained soils of urban area: Field tests and FEA modelling. *Tunn. Undergr. Space Technol.* **2021**, *111*, 103857. [CrossRef]